Hydro-Acoustics of Inflow-Stator-Rotor Interaction in Submersed Elastic Duct with Ribs

Hafiz M. Atassi
University of Notre Dame,
Notre Dame, Indiana, 46556

Overview

- Background
- Objectives
- Approach
- Results
- Major Accomplishments
- Significance
- Future Work

Sound Radiation from Rotor Blades Interaction with Turbulent and Swirling Motion

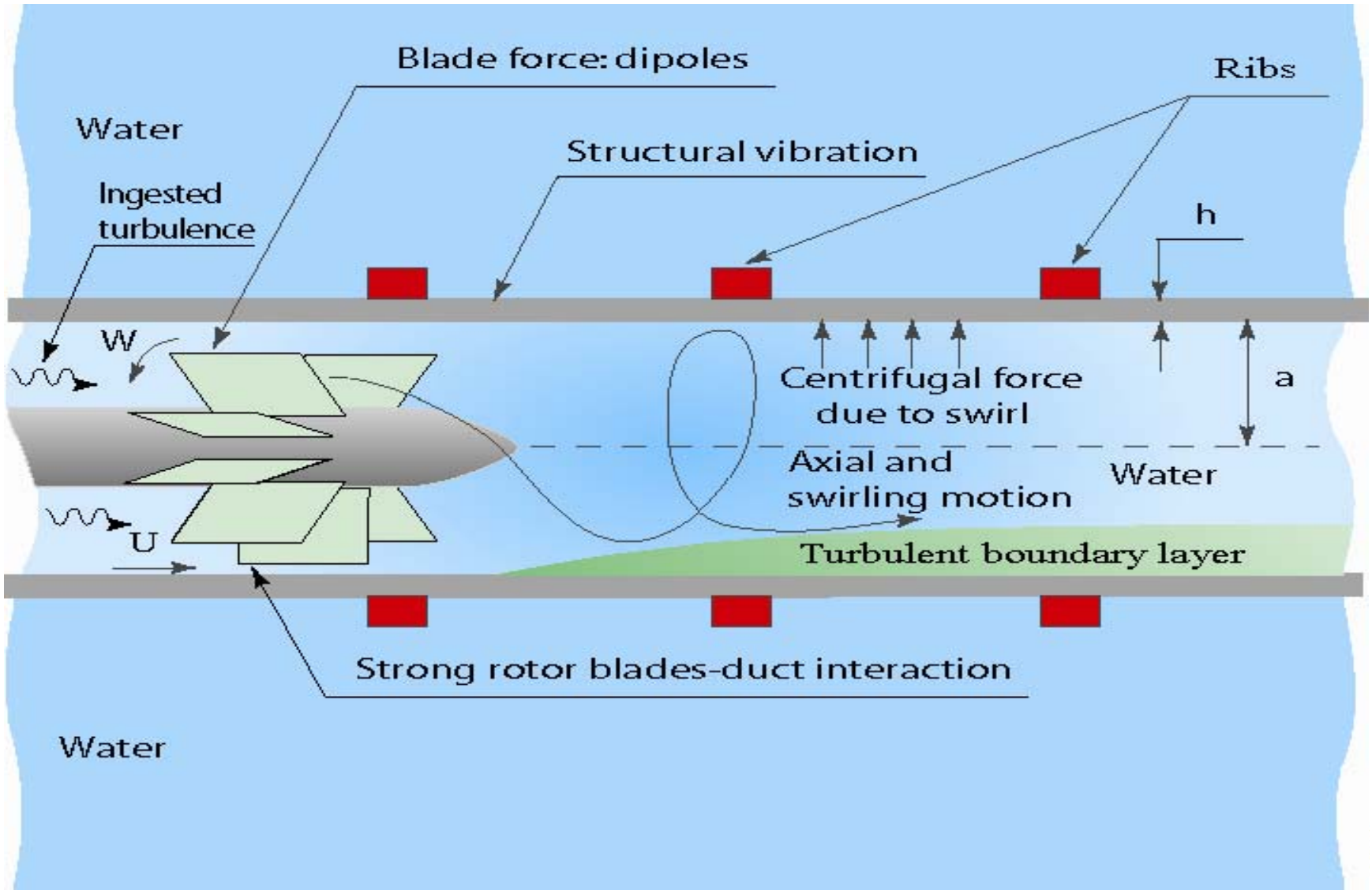

CLASSICAL APPROACH

1. Flow-Propeller interaction is modeled with rigid walls and yields the hydrodynamic forces and the equivalent blocked dipole strength.
2. Compact blocked dipoles in elastic duct are used to yield the radiated sound.

- This approach does not account for:
  - the coupling between the flow and the elastic duct which affects the strength of the hydrodynamic forces and the modeling of the radiated sound.
  - The spatially distributed nature of the flow dipoles.
  - The duct additional dipoles arising from propeller wall interaction.

Questions:

Hydrodacoustics:
How Does the Elastic Duct Change the Fluctuating Hydrodynamic Pressure Along the Propeller Blade?

Structural Acoustics :
How Does Coupling the Elastic Duct to Inflow Nonuniformities Change the Equivalent Source Strength and the Far-Field Acoustic Radiation?

Answering these questions suggests:
an interdisciplinary approach combining hydroacoustics and structural acoustics.

OBJECTIVES

- Model Coupled Swirling Nonuniform Flow Interaction with a Propeller in Elastic Duct:
  - Quantify Effects of Flexible Duct on the Blade Equivalent Dipole Strength and the Far-Field Radiated Sound.
  - Examine Noise Generating Mechanisms Due to the Flexible Duct Motion.
- Determine and Characterize Sound Sources in Elastic Ducts:
  - Localized Sources.
  - Distributed Sources.
- Model Transfer Functions for Sound Radiation from Ducted Fluid-Structure Interactions.
- Extend Model to Ducts with Control Ribs.
- Validate Model by Comparison with Experiments.

Coupled Fluid-Duct Predictive Model

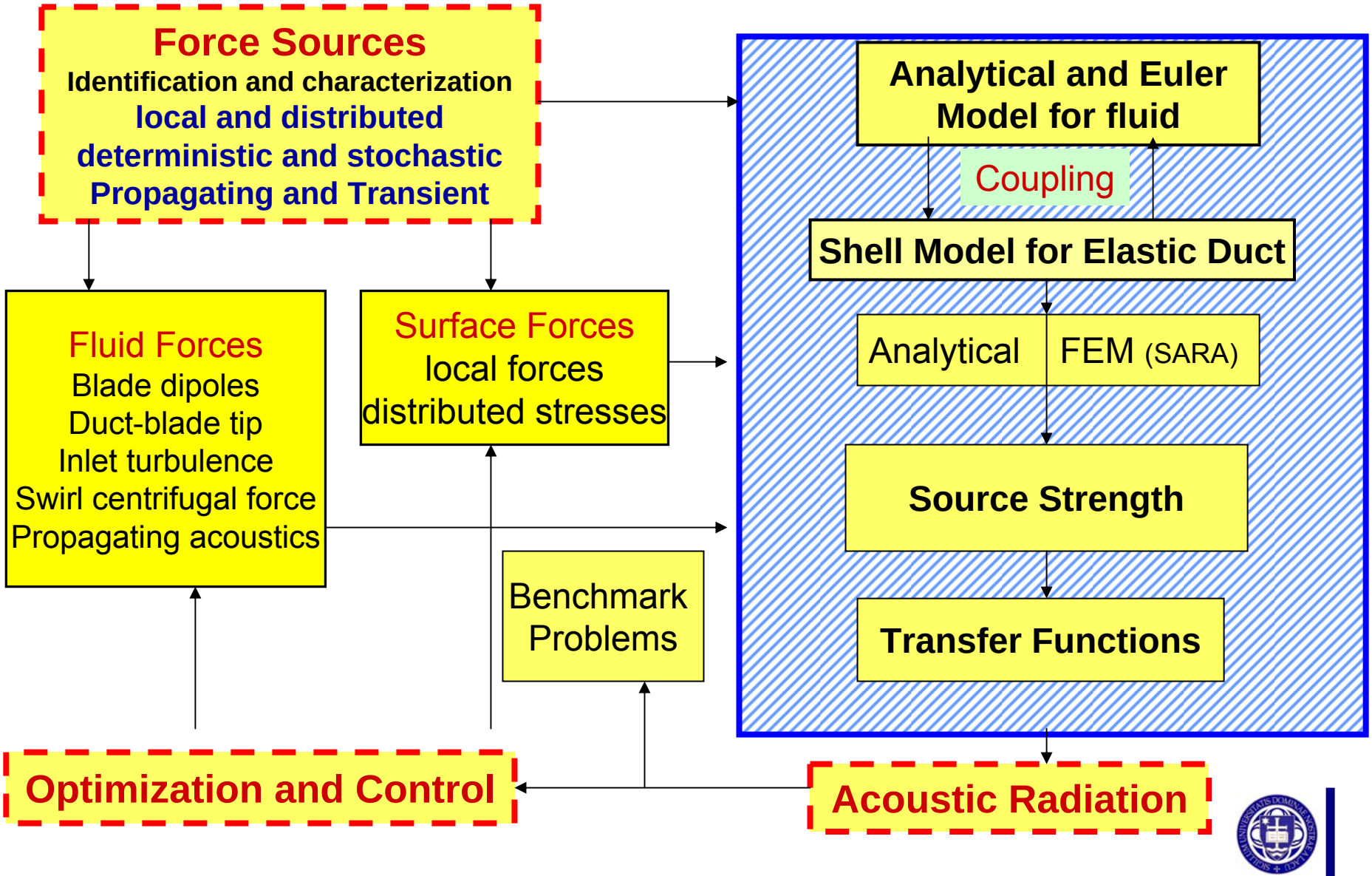

ISSUES FOR CONSIDERATION

- Coupling the propeller with the system:
  - How does coupling the elastic duct to the swirling fluid motion affect the blade and duct hydrodynamic forces: local and distributed dipole strength?
  - How do the strength and orientation of the dipole sources affect the duct hydrodynamic forces.
  - How important are transient forces extending over a length of the order of the duct radius a ? How do they compare with the duct mode shapes? Do they lead to strong non-compact source effects? If so, what are these effects?
  - Deterministic versus stochastic excitations?
- Propeller in free space versus propeller in duct:
  - Different mechanisms for propeller in duct with free-space propeller?
- Effect of Ribs and Duct Material:
  - How does coupling with ribs affect the scattering mechanism?
  - How does the swirling flow interacts with ribs?
  - How strong is the coupling between pressure and vortical modes?

Coupling the Propeller with the Shell

$$\vec{V}(\vec{x},t) = \vec{U}(\vec{x}) + \vec{u}^{(R)}(\vec{x},t) + \vec{u}^{(S)}(\vec{x},t)$$

Rigid Wall

$$\mathcal{L}_f \vec{u}^{(R)} = 0$$

$$(u_r^{(R)})_{r_h} = 0$$

$$(u_r^{(R)})_{r_t} = 0$$

$$\vec{u}_{in}^{(R)} = \vec{u}_g$$

$$IOBC$$

Flexible Wall

$$\mathcal{L}_f \vec{u}^{(S)} = 0$$

$$(u_r^{(S)})_{r_h} = 0$$

$$(u_r^{(S)})_{r_t} = \frac{D_o}{Dt}\varsigma_r$$

$$\mathcal{L}_S \vec{\varsigma} = P_h + P_S$$

$$(\mathcal{L}_S - \mathcal{L}_W)\vec{\varsigma} = P_h$$

$$\vec{u}_{in}^{(S)} = 0$$

$$IOBC$$

Equations for Isotropic Elastic Shell

- The equations for the axial, circumferential and radial displacements are

$$L_S = \begin{pmatrix} L_{11} & L_{12} & L_{13} \\ L_{21} & L_{22} & L_{23} \\ L_{31} & L_{32} & L_{33} \end{pmatrix} \begin{pmatrix} \varsigma_x \\ \varsigma_\theta \\ \varsigma_r \end{pmatrix} = \begin{pmatrix} F_x \\ F_\theta \\ F_r \end{pmatrix}$$

$$\mathcal{L}_{11} = -E_1\left(\frac{\partial^2}{\partial x^2} + \frac{1-\nu}{2a^2}\frac{\partial^2}{\partial \theta^2}\right) + \rho_s h\frac{\partial^2}{\partial t^2} \qquad \mathcal{L}_{12} = -E_1\frac{1+\nu}{2a}\frac{\partial^2}{\partial x \partial \theta} = \mathcal{L}_{21}$$

$$\mathcal{L}_{13} = -E_1\frac{\nu}{a}\frac{\partial}{\partial x} = -\mathcal{L}_{31} \qquad \mathcal{L}_{22} = -E_1\left(\frac{(1-\nu)(1+4\beta^2)}{2}\frac{\partial^2}{\partial x^2} + \frac{1+\beta^2}{a^2}\frac{\partial^2}{\partial \theta^2}\right) + \rho_s h\frac{\partial^2}{\partial t^2}$$

$$\mathcal{L}_{23} = -E_1\left(\frac{1}{a^2}\frac{\partial}{\partial \theta} - \beta^2(2-\nu)\frac{\partial^3}{\partial \theta \partial x^2} - \frac{\beta^2}{a^2}\frac{\partial^3}{\partial \theta^3}\right) = -\mathcal{L}_{32}$$

$$L_{33} = E_1\left(\frac{1}{a^2} + \beta^2 a^2\frac{\partial^4}{\partial x^4} + \frac{\beta^2}{a^2}\frac{\partial^4}{\partial \theta^4} + 2\beta^2\frac{\partial^4}{\partial x^2 \partial \theta^2}\right) + \rho_s h\frac{\partial^2}{\partial t^2}$$

Fourier Transform of the Equations

$$F(x,r,\theta) = \frac{1}{2\pi} \sum_{m=-\infty}^{m=+\infty} e^{im\theta} \int_{-\infty}^{+\infty} \tilde{F}(r,m,\alpha) e^{i\alpha x} d\alpha$$

$$\tilde{F}(r,m,\alpha) = \frac{1}{2\pi} \sum_{m=-\infty}^{m=+\infty} e^{-im\theta} \int_{-\infty}^{+\infty} F(x,r,\theta) e^{-i\alpha x} dx d\theta$$

Modal Equations for Isotropic Water-filled Elastic Shell

$$S=\begin{pmatrix} S_{11} & S_{12} & S_{13} \\ S_{21} & S_{22} & S_{23} \\ S_{31} & S_{32} & S_{33} \end{pmatrix}\begin{pmatrix} \tilde{\varsigma}_x \\ \tilde{\varsigma}_\theta \\ \tilde{\varsigma}_r \end{pmatrix}=\begin{pmatrix} \tilde{\mathcal{F}}_x \\ \tilde{\mathcal{F}}_\theta \\ \tilde{\mathcal{F}}_r \end{pmatrix} \qquad \tilde{R}=s^{-1}$$

$$S_{11}=E_1\left[\alpha^2+\frac{m^2(1-\nu)}{2a^2}\right]-\omega^2\rho_s h$$

$$S_{12}=E_1(1+\nu)\frac{m\alpha}{2a}=L_{21}$$

$$S_{13}=-iE_1\nu\frac{\alpha}{a}=-S_{31}$$

$$S_{22}=E_1\left[\frac{(1-\nu)\alpha^2}{2}+\frac{m^2}{a^2}\right]+E_1\left[2\alpha^2\beta^2(1-\nu)+\frac{\beta^2m^2}{a^2}\right]-\omega^2\rho_s h$$

$$S_{23}=-E_1\left[\frac{m}{a^2}+\beta^2(2-\nu)\alpha^2 m+\frac{\beta^2m^3}{a^2}\right]i=-S_{32}$$

$$S_{33}=E_1\left(\frac{1}{a^2}+\beta^2a^2\alpha^4+\frac{\beta^2m^4}{a^2}+2\beta^2m^2\alpha^2\right)$$

$$-\omega^2\rho_s h+\rho_1\omega^2\frac{H_m^{(1)}(\mu_1 a)}{\mu_1 H_m^{'(1)}(\mu_1 a)}-\rho_2\omega^2\frac{J_m(\mu_2 a)}{\mu_2 J_m^{'}(\mu_2 a)}$$

$\Downarrow$

Internal Fluid loading will be modified by nonuniform fluid motion and duct ribs.

Scaling of Forces

Reduced Frequency $\omega^* = \omega\, a/c_0$	Elastic Eh/a^2 1	Du ct Inertia $\rho_s \omega^2 h$ $(\rho_s c_0^2/E)\, \omega^{*2}$	Fluid Loading $\rho_w \omega c_0$ $(\rho_w c_0^2/E)(a/h)\omega^*$
$\omega^* << 1$	1	$\approx 0.1\omega^{*2}$	$\approx 2\ \omega^*$
$\omega^* \approx 1$	1	0.1	≈ 2
$\omega^* >> 1$	1	$\approx 0.1\ \omega^{*2}$	$\approx 2\ \omega^*$

The Shell Radial Displacement

$$\tilde{R} = \{\tilde{R}_{ij}\} = S^{-1}$$

$$\tilde{\zeta} = \tilde{R}\tilde{F}$$

$$\tilde{F} = \{0, 0, \tilde{F}_r\}^t$$

$$\tilde{\zeta} = \{0, 0, \tilde{\zeta}_r\}^t$$

$$\tilde{\zeta}_r = \tilde{F}_r \, \tilde{R}_{33}$$

We assume that $\tilde{R}_{33}$ can be expanded into a **rational fraction in** α. The shell radial displacement ζ_r can then be obtained as a convolution integral of the external force F_r with the modes of the shell motion.

The Shell Radial Displacement Cont'd

$$\tilde{\varsigma}_r = \tilde{P}_h \tilde{R}_{33}$$

$$\tilde{R}_{33} = \sum_{\alpha_\ell} \frac{A_\ell}{\alpha - \alpha_\ell}$$

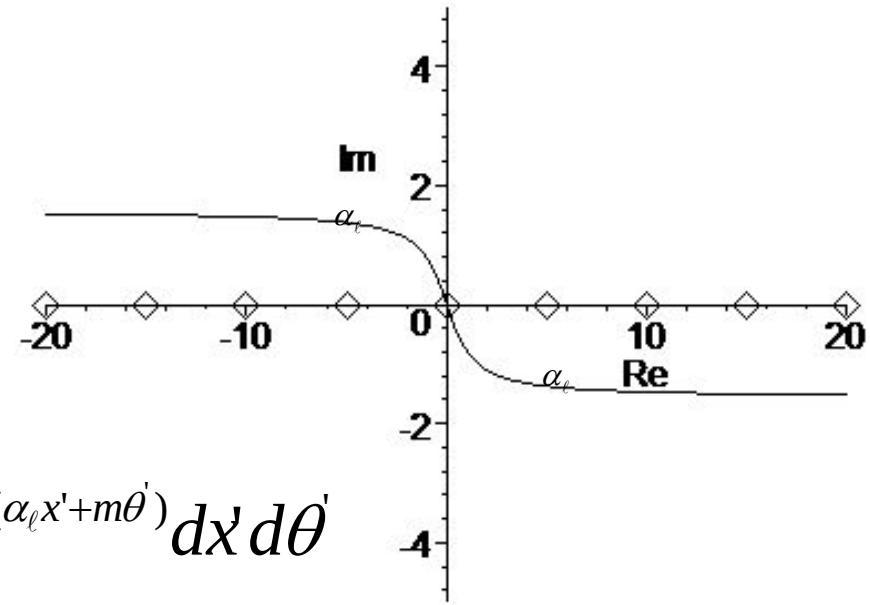

$$\varsigma_r = \sum_{\ell,m} e^{i(\alpha_\ell x + m\theta - \omega t)} \int_{-\infty}^{x} \int_{0}^{2\pi} P_h(x', \theta', \omega) e^{-i(\alpha_\ell x' + m\theta')} dx' d\theta'$$

$$\varsigma_r = \text{Propagating} \; + \; \textit{Transient}$$

Damping is introduced by deforming contour of integration in the complex α -plane

$$(\varsigma_r)_{prop} = \sum_{\ell,m} e^{i(\alpha_\ell x + m\theta - \omega t)} \tilde{P}_h(\alpha_\ell, m, \omega)$$

Results suggested from the theory

- For local excitation forces (blade tip-gap-wall interaction), the “water filled” shell modes are excited and radiate sound outside the duct.

- For distributed excitation forces (acoustic or hydrodynamic), the duct wall motion is modulated by the excitation forces.

How Will The Ribs Affect The Hydro-Structural Acoustics Interaction

- The ribs will act as scatterers causing standing waves in the duct.
- $\tilde{R}_{33}$ must be expanded into rational fraction with periodicity leading to an infinite series.
- The dispersion relation (ω vs α) will exhibit this periodicity and a new interaction mechanism will take place between almost convecting hydrodynamic disturbances (wakes, turbulence) with the elastic duct.
- This suggests: (1) enhanced interaction, (2) non-compact source effects and (3) strong acoustic directivity patterns.

Dispersion relations for an aluminum duct with ribs and with no ribs.

m=0, rib spacing: d=a, thickness of the shell: h=0.01a.

No ribs

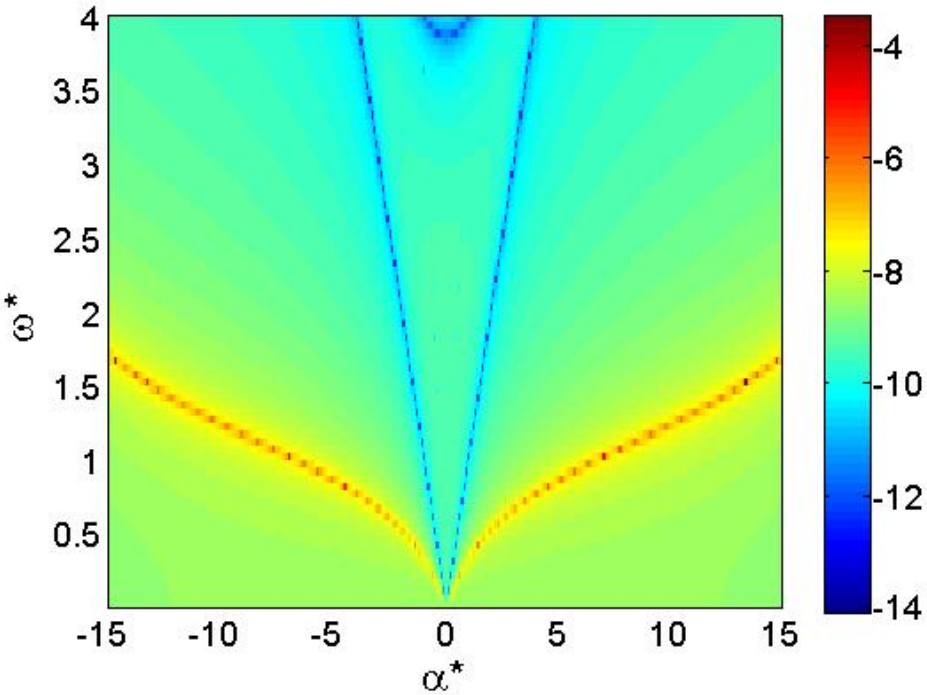

With ribs

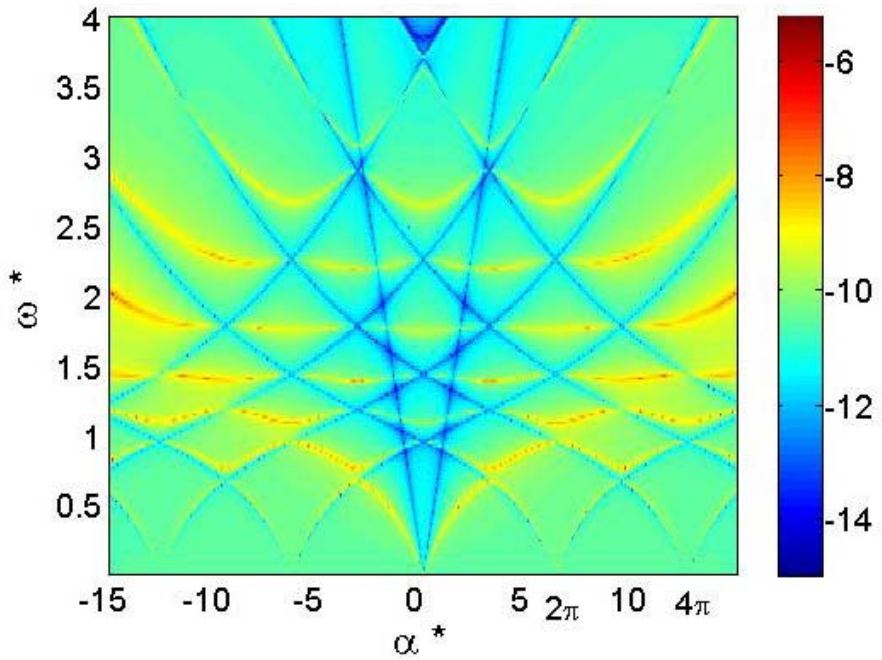

Dispersion relations for an aluminum duct with ribs and with no ribs.

m=1, rib spacing: d=a, thickness of the shell: h=0.01a.

No ribs

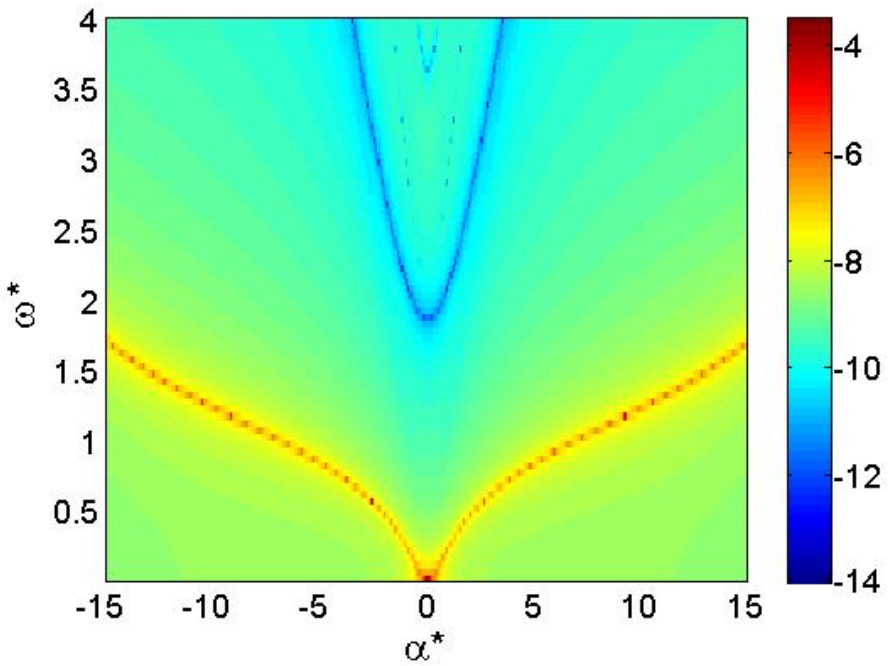

With ribs

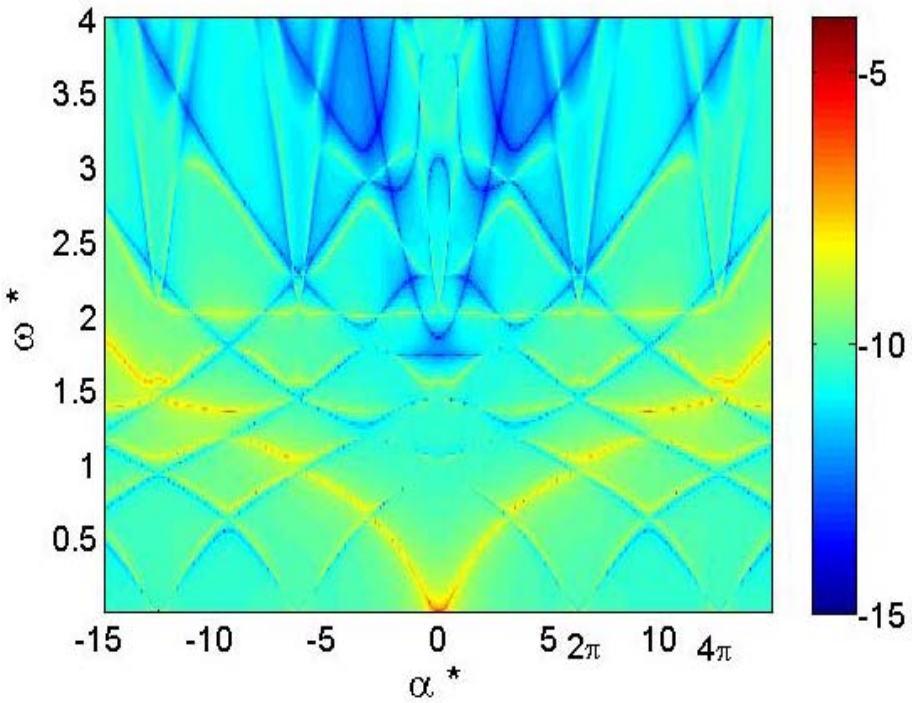

Dispersion relations of an aluminum duct with ribs.

Rib spacing: d=a, thickness of the shell: h=0.01a.

m=5

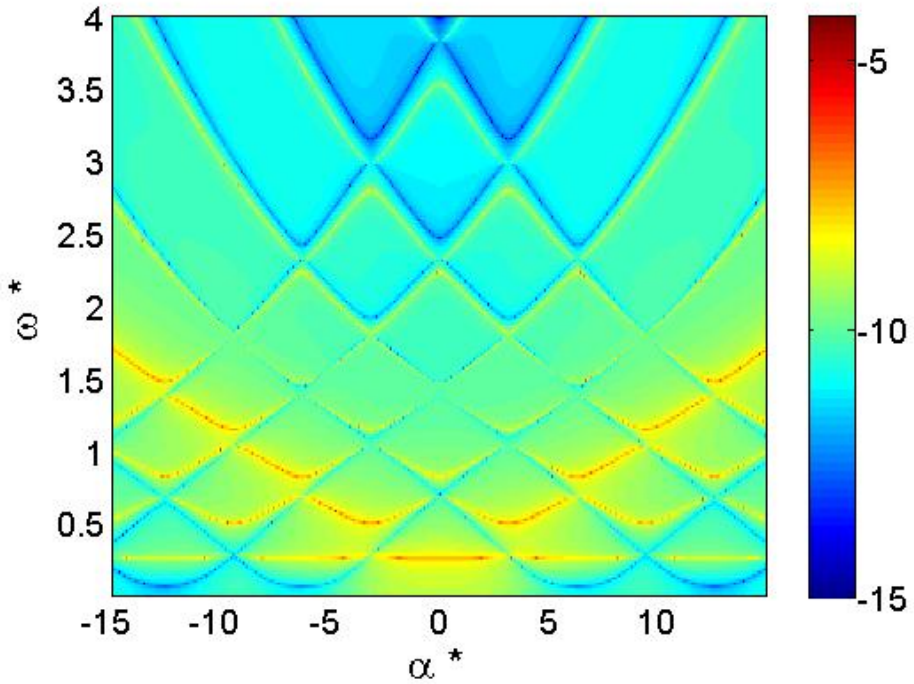

m=8

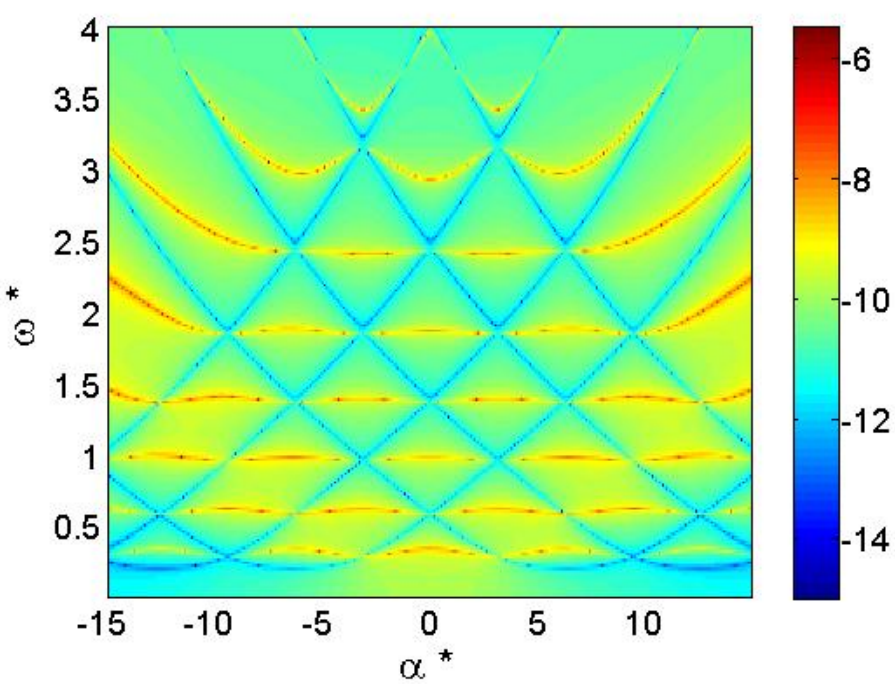

Coordinates System

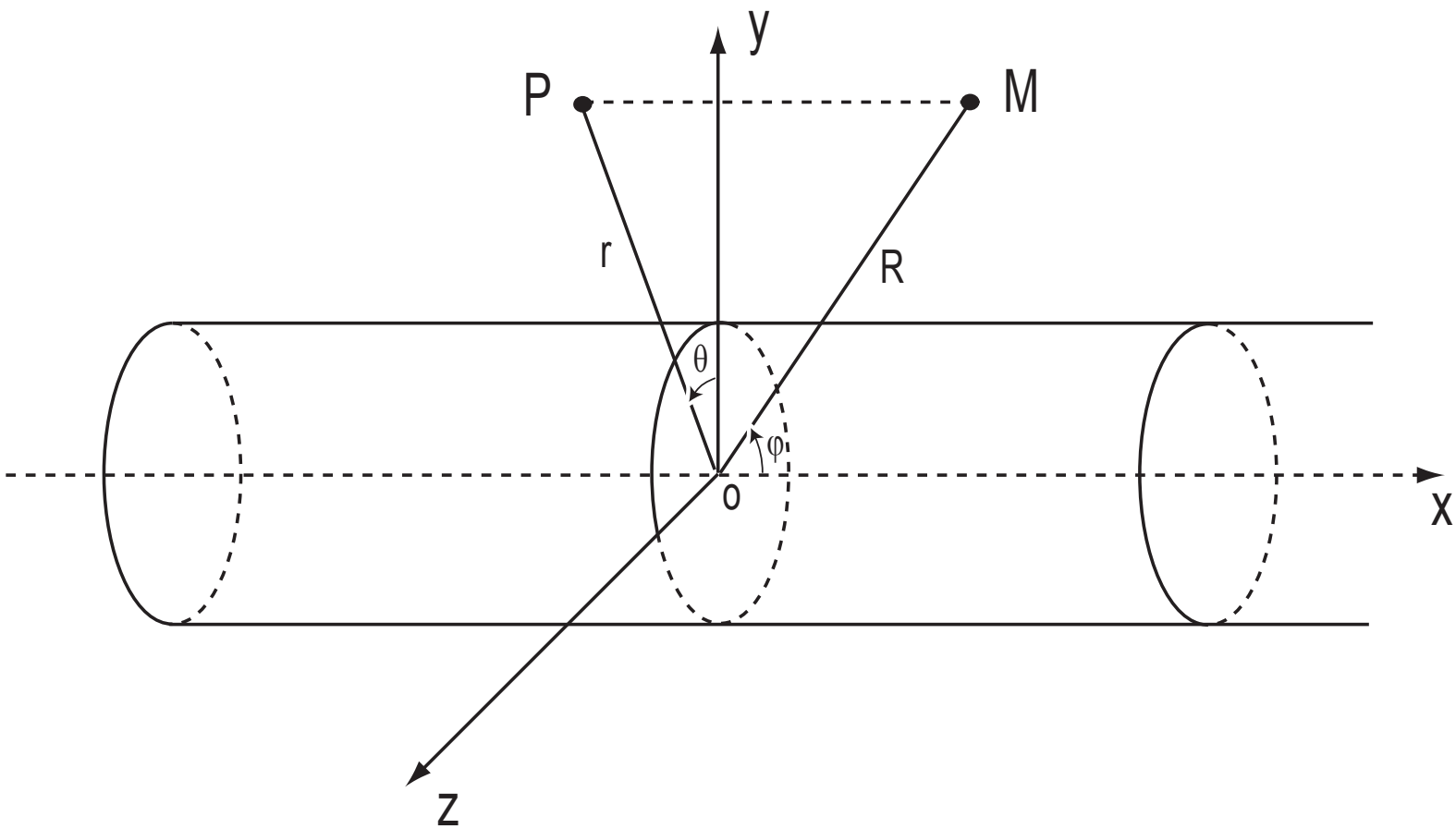

The far field acoustic pressure in terms of duct displacement.

$$P = \frac{-i\rho\omega^2 e^{ikR}}{\pi kR \sin\varphi} \sum_{m=-\infty}^{m=+\infty} \frac{(-i)^{|m|} \varsigma_r(m, \omega^* \cos\varphi)}{H'_{|m|}(\omega^* \sin\varphi)} e^{im\theta}$$

ς_r is the radial displacement of the duct. $\alpha^*=\omega^*\cos\varphi$ is the stationary phase wave number ➔ acoustically relevant dispersion relation ω^* vs α^* is such $|\alpha^*| < \omega^*$.

Dispersion relation of an aluminum duct with steel ribs for m=0. Rib spacing: d=a, thickness of the shell: h=0.01a.

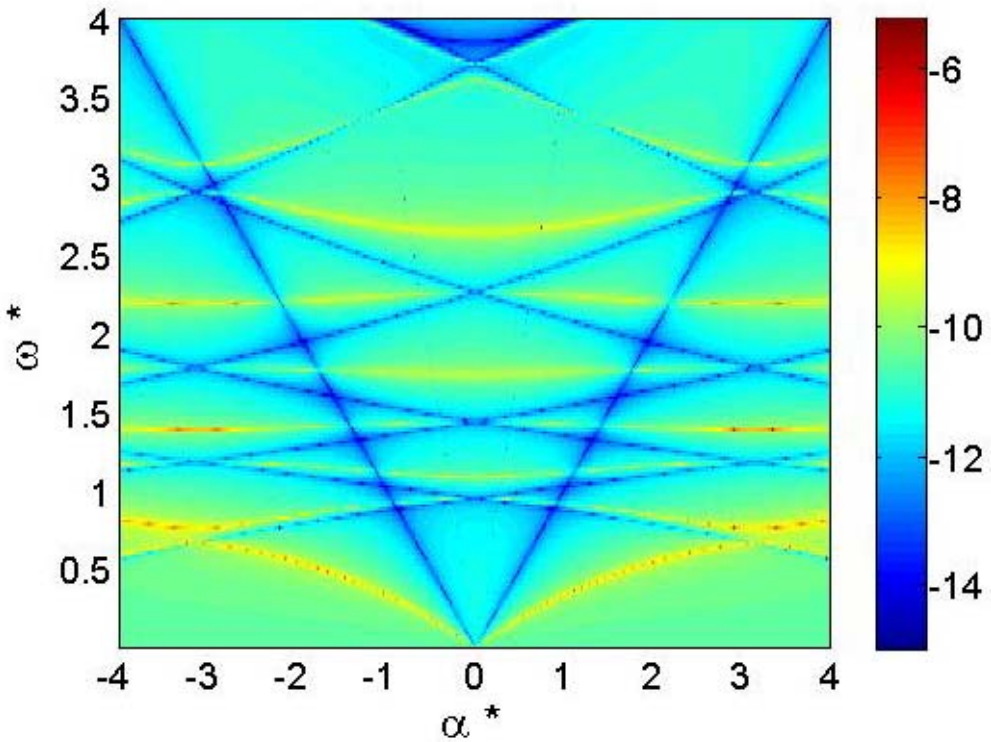

Benchmark Analytical Solutions

Distributed and Local Excitation Sources

1. Plane Wave
2. Single Force
3. Dipole

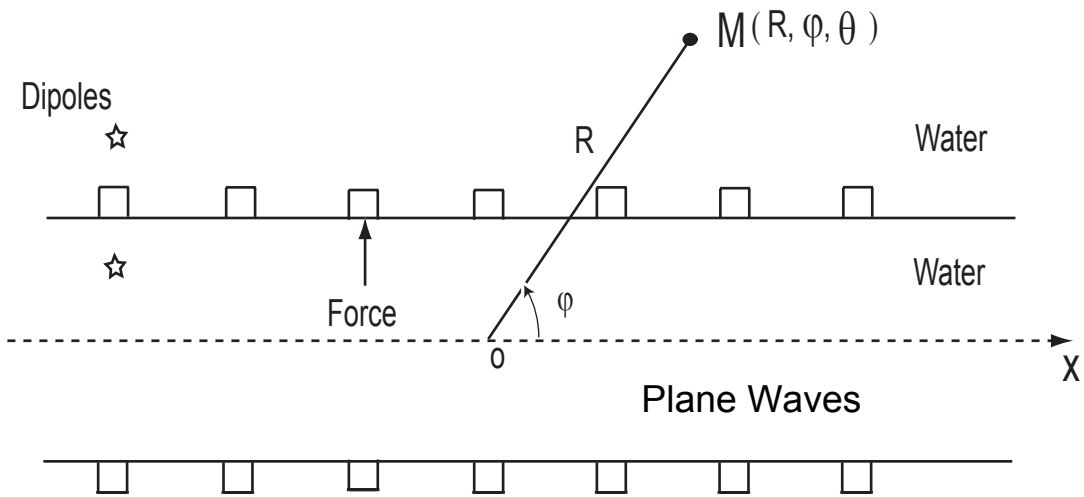

Benchmark Analytical Solutions

Distributed and Local Excitation Sources

- Plane acoustic waves in duct:(distributed)
  - Examine elastic duct effects on transfer function for different materials.
  - An almost universal transfer function

$$\frac{(rp_r')}{\bar{p}_i} = K\left(\frac{\rho_w}{\rho_s}\frac{a}{h}\right)\Pi(\omega^*, \omega_s, \beta, \nu)$$

$$\omega^* = \frac{\rho_w \omega}{c_w}, \quad \omega_s = \frac{\rho_s \omega}{c_p}$$

$$\beta^2 = \frac{h^2}{12a^2}, \quad c_p = \sqrt{\frac{E}{\rho_s(1-\nu^2)}}$$

- Blade tip interaction with duct:(local)
  - Force is almost local but not stationary.

$$p_d = \frac{f_r}{a}\delta(x - x_0)\sum_{s=1}^{s=B}\delta(\theta - \frac{2\pi s}{B} + \Omega t)$$

	ρ_s	E	ν	c_p
Steel	7700	0.195×10^{12}	0.290	5258
Aluminum	2700	0.7×10^{11}	0.33	5394
Hard Rubber	1100	0.2×10^{10}	0.4	1471

Transfer Function Π for Propagating Acoustic Waves in water filled and submerged duct

$$\frac{(rp_r^{'})}{\overline{p}_i} = K\left(\frac{\rho_w}{\rho_s}\frac{a}{h}\right)\Pi,$$

$$\Pi = \frac{\omega_s^{\,2}\left(\omega^{*^2} - \omega_s^{\,2}\right)}{\left(\omega^{*^2} - \omega_s^{\,2}\right)\left[\left(1+\beta^2\omega^{*^2}\right) - \omega_s^{\,2}\right] - \nu^2\omega^{*^2}}$$

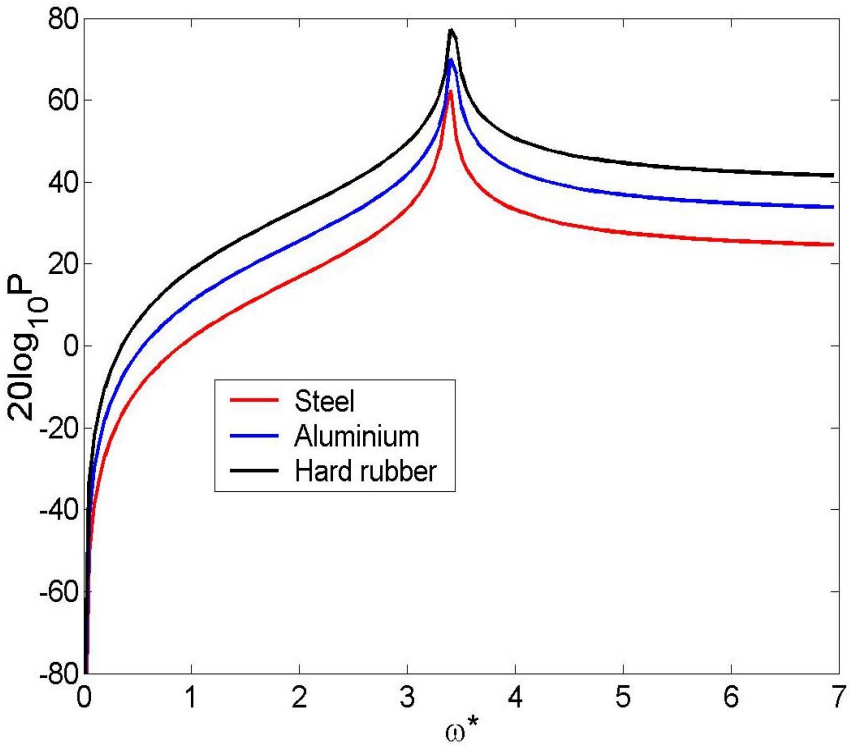

Dimensional Form

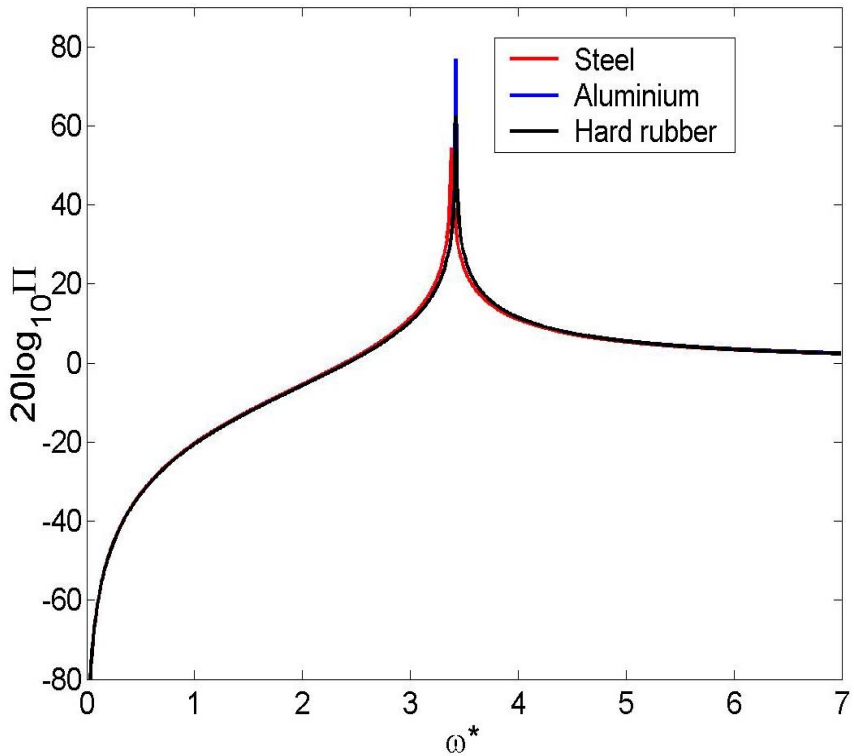

Non-Dimensional Form

Axisymmetric modal (m=0) radial displacement of the duct surface vs ω * in response to a single force (θ=0, φ=π/2)

φ=π/2, θ=0.

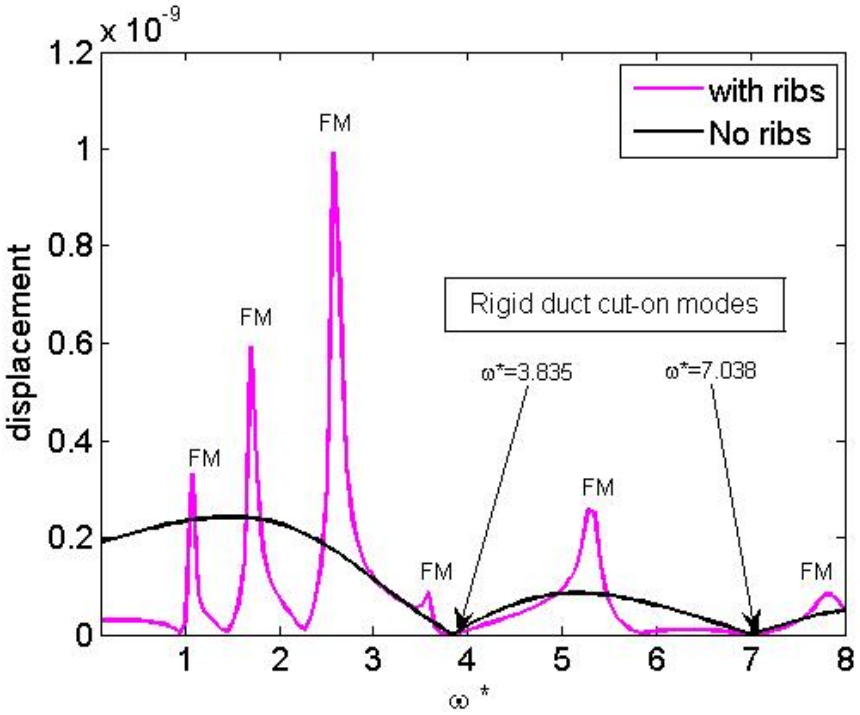

φ=π/4, θ=0.

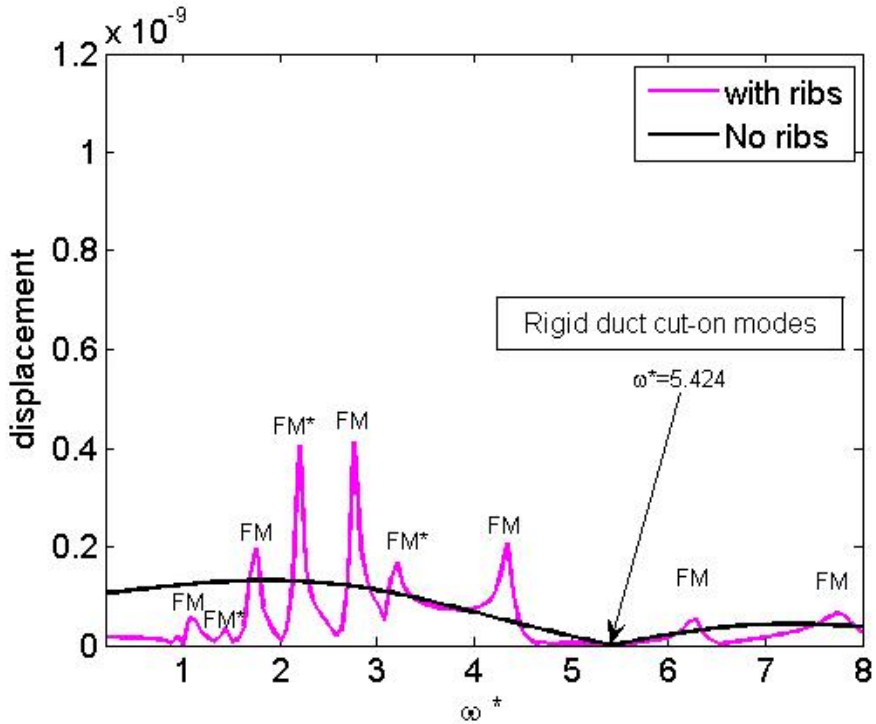

Sound level of the axisymmetric mode (m=0) vs ω* in response to a single force(θ=0, φ=π/2).

φ=π/2, θ=0

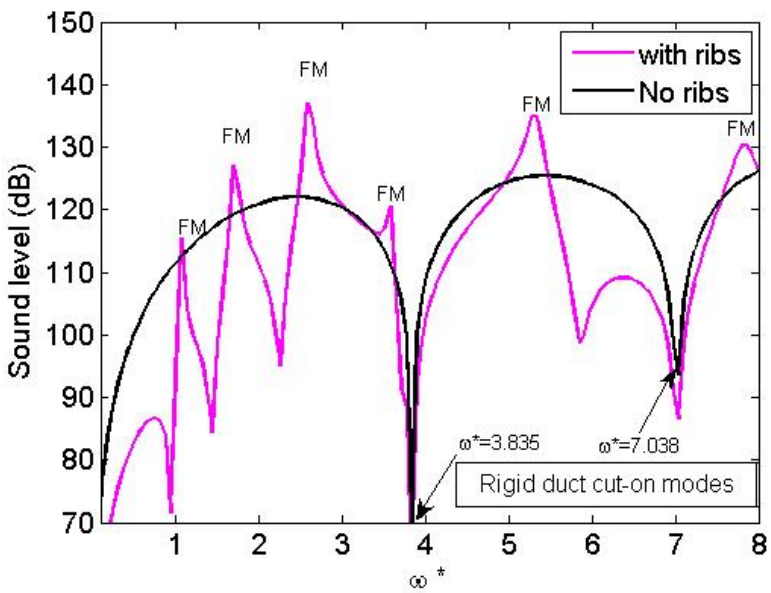

φ=π/4, θ=0

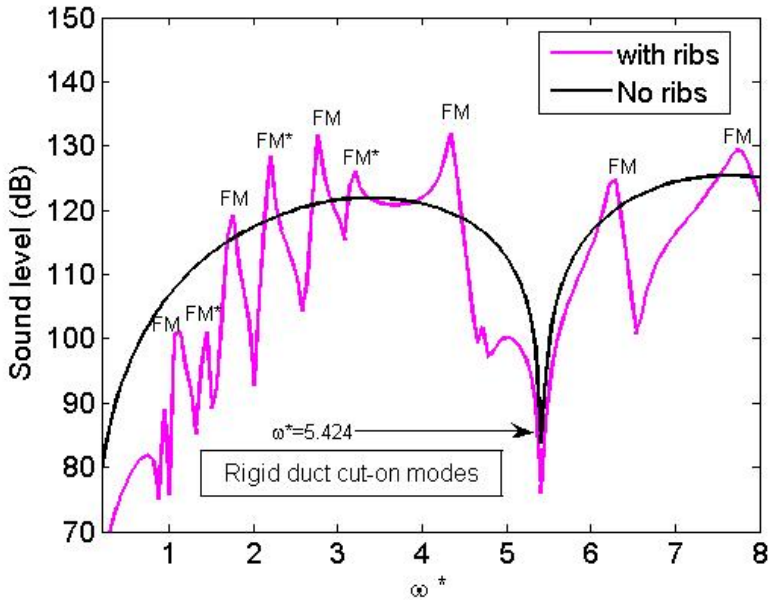

Modal (m=1) radial displacement of the duct surface vs ω * in response to a single force (θ=0, φ=π/2)

φ=π/2, θ=0

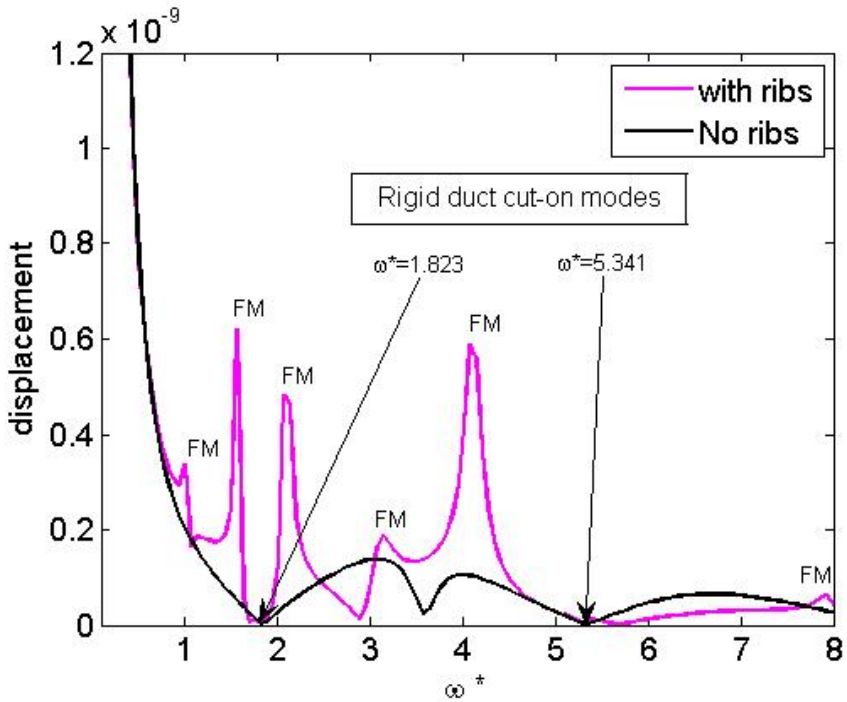

φ=π/4, θ=0

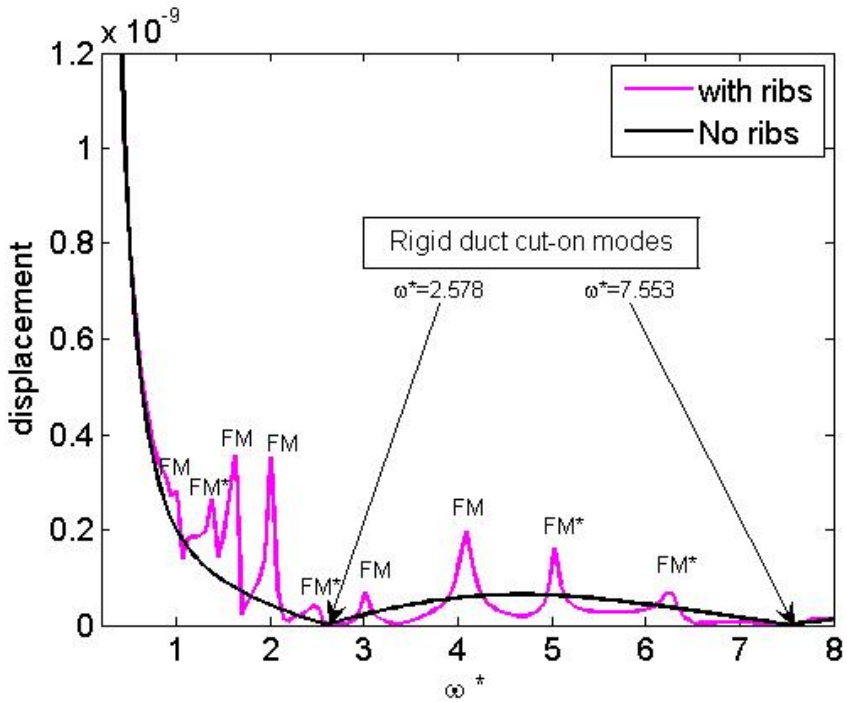

Modal (m=1) sound level vs ω* in response to a single force(θ=0, φ=π/2).

φ=π/2, θ=0

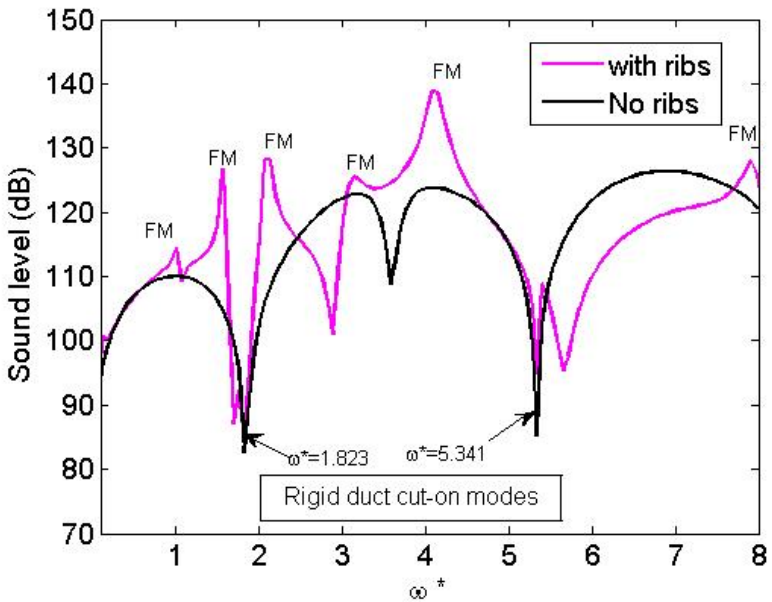

φ=π/4, θ=0

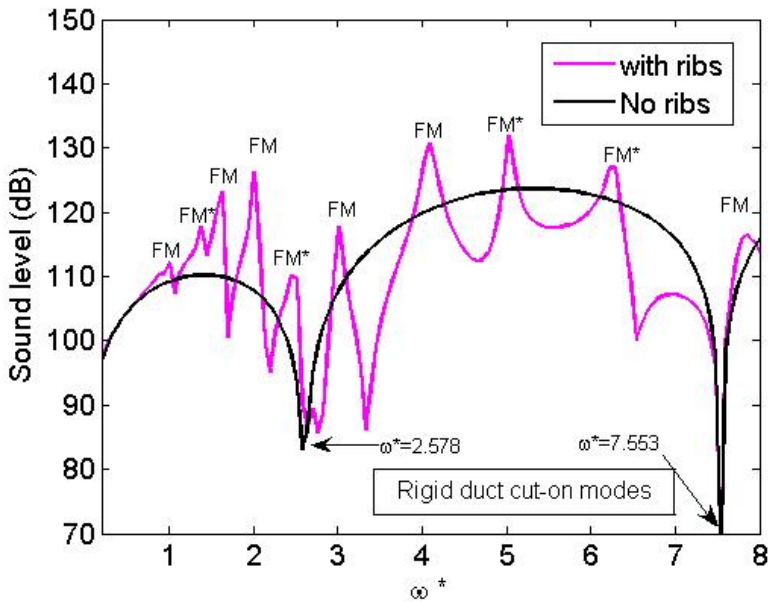

Total sound level vs ω* in response to a single force (θ=0, φ=π/2).

φ=π/2, θ=0

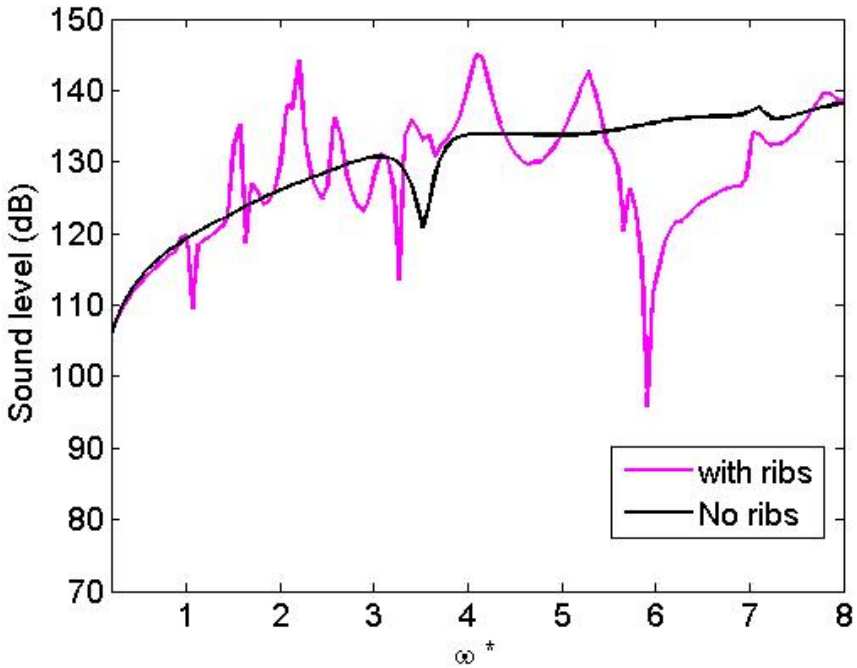

φ=π/4, θ=0

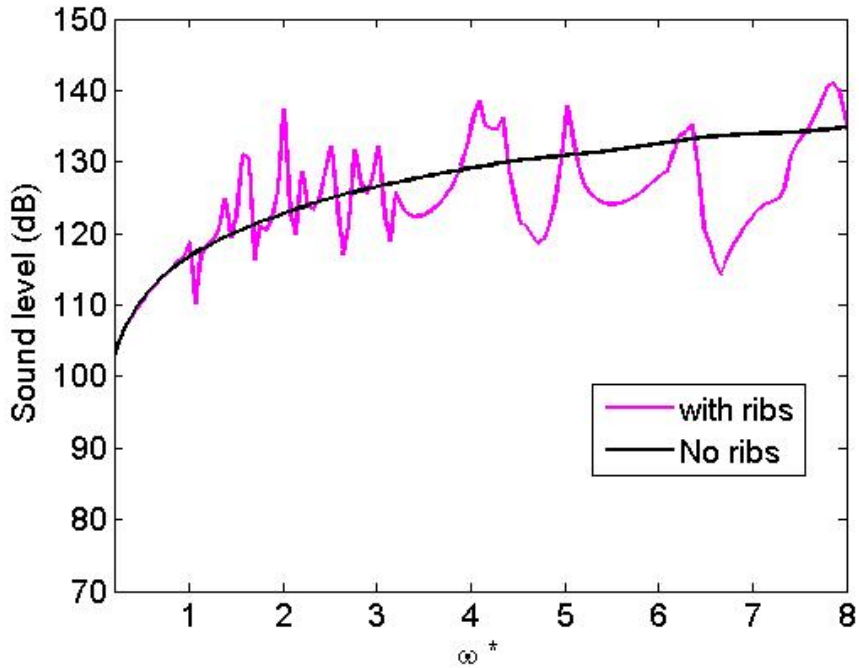

Sound level directivity in response to a single force at θ=0, φ=π/2.

$\omega^* = 0.5$

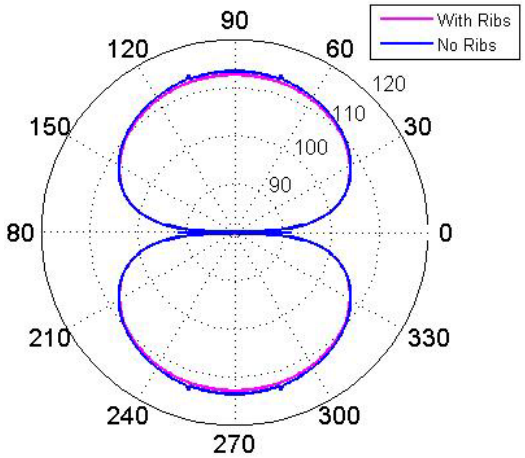

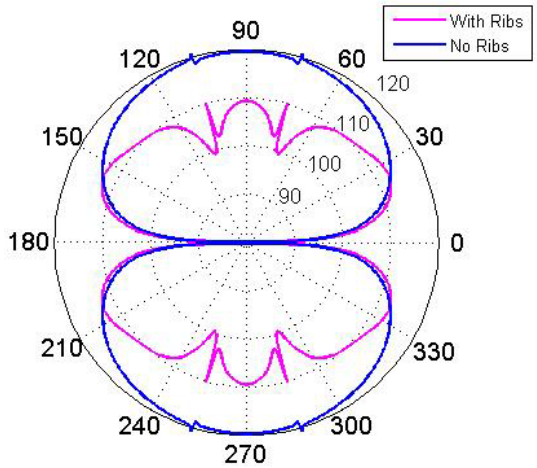

$\omega^* = 1.069$

$\omega^* = 2$

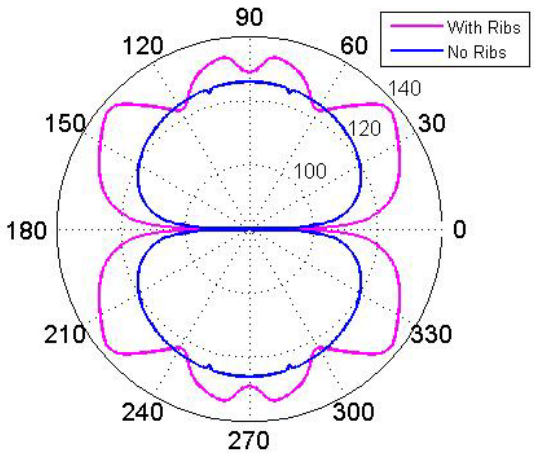

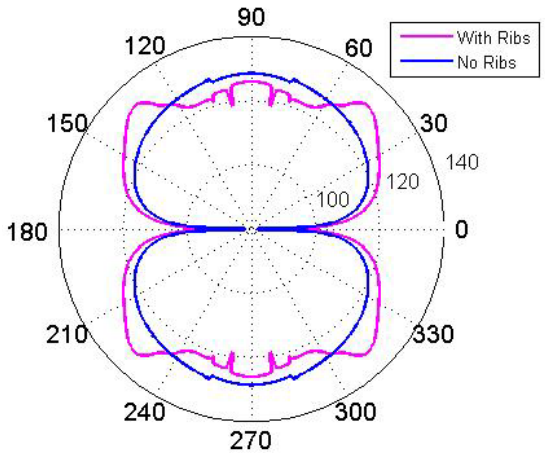

$\omega^* = 2.5$

Dipole Acoustic Radiation through a Flexible Shell

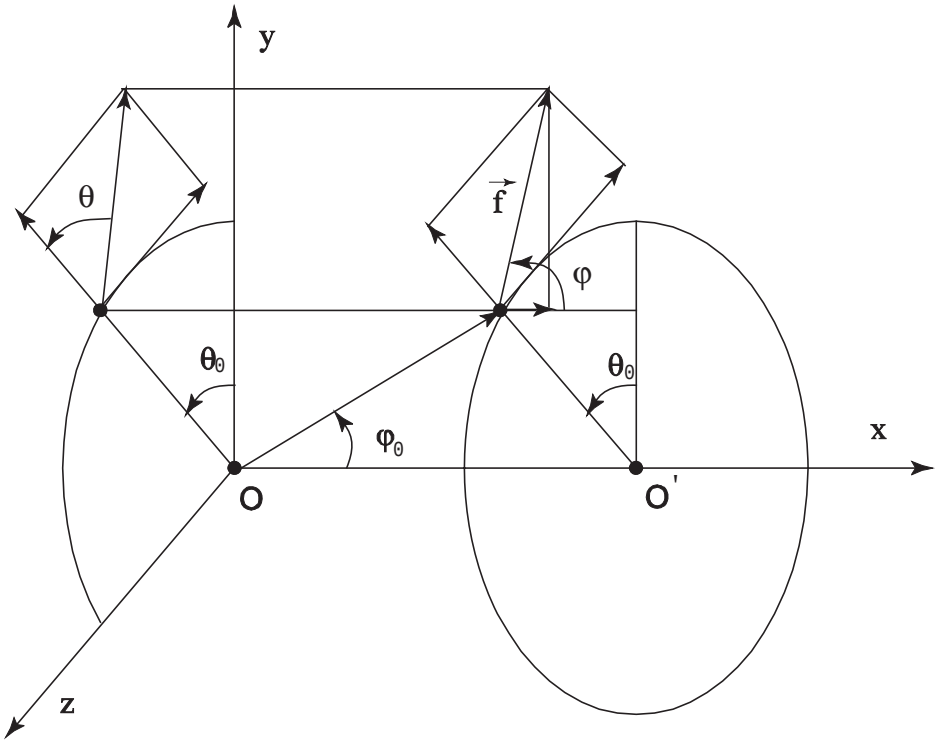

A Dipole of strength f may have axial, radial and circumferential components

Aluminum Duct, a=1m, h=1cm. Reduced frequency, $\omega^* = \omega a / c_0$

Results are normalized to free dipole

Far field sound level in response to an axial dipole. The far field observation point is at φ=π/4.

axial dipole located at r_0=0.5a

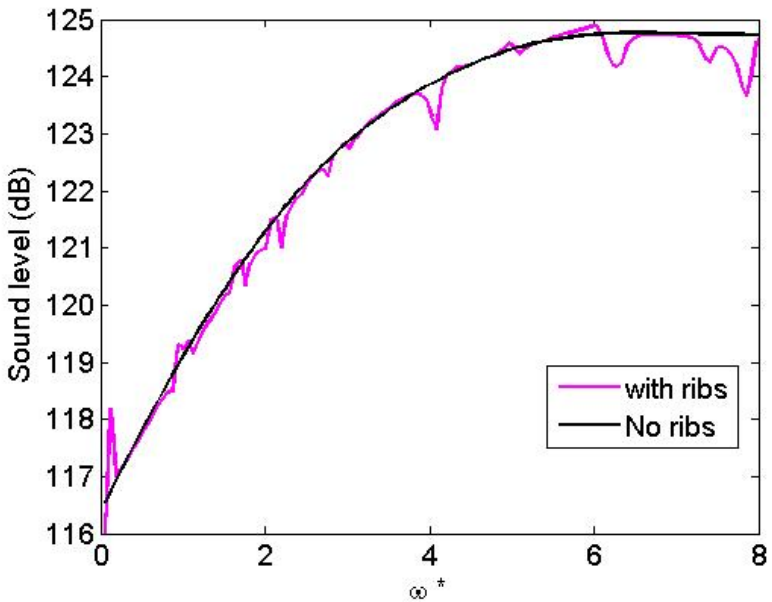

axial dipole located at r_0=0.8a

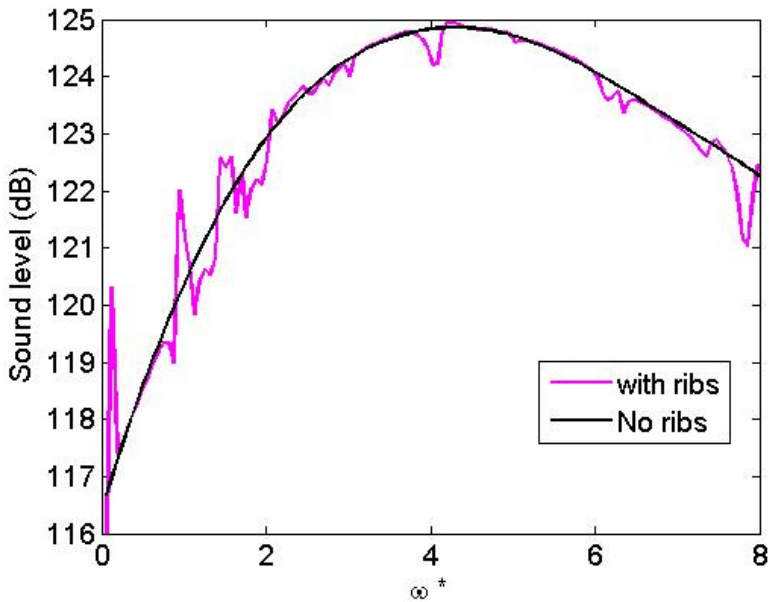

Far field sound level in response to a radial dipole. The far field observation point is at φ=π/2.

radial dipole located at r_0=0.5a

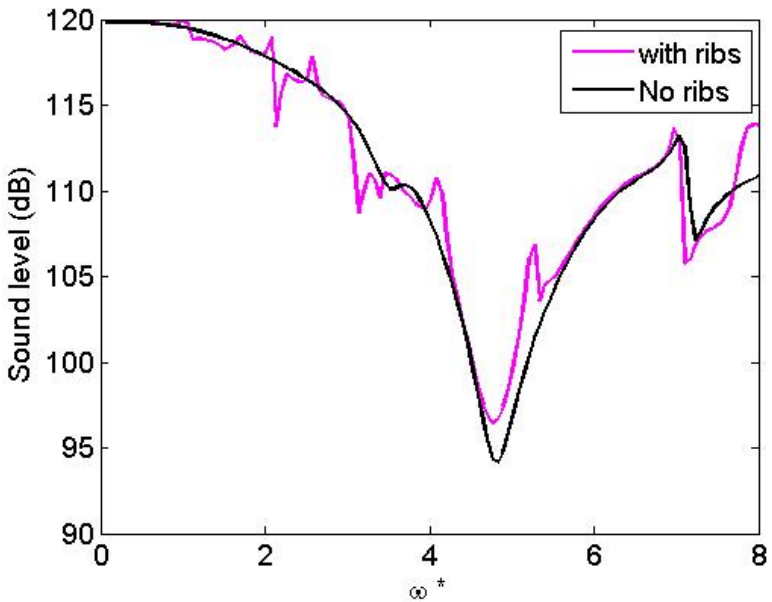

radial dipole located at r_0=0.8a

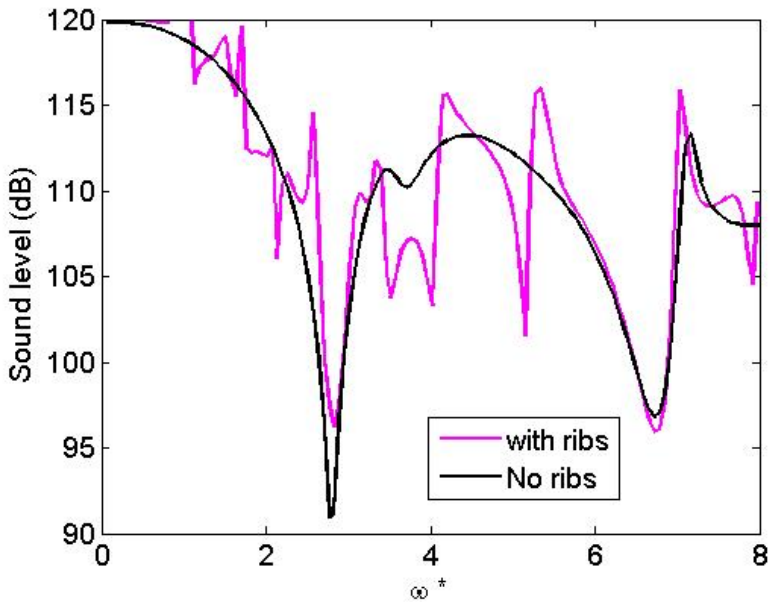

Far field sound level in response to a circumferential dipole. The far field observation point is at φ=π/2.

circumferential dipole located at r_0=0.5a

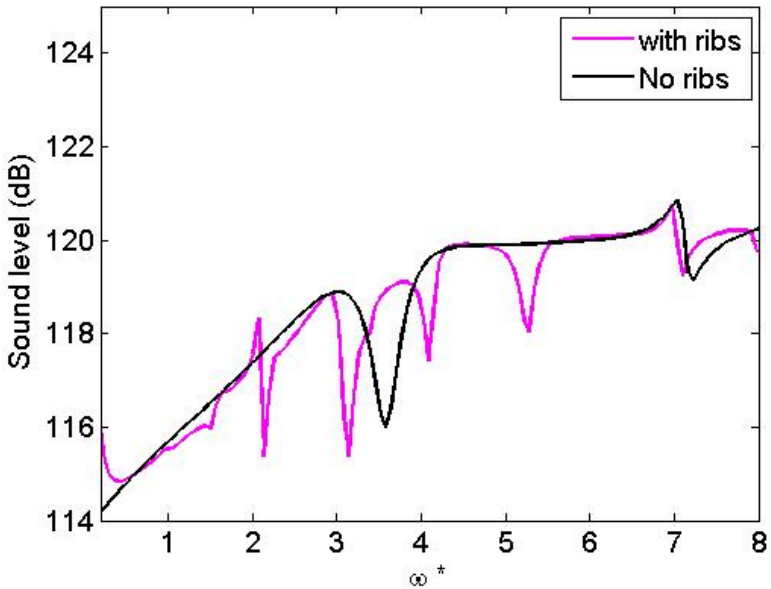

circumferential dipole located at r_0=0.8a

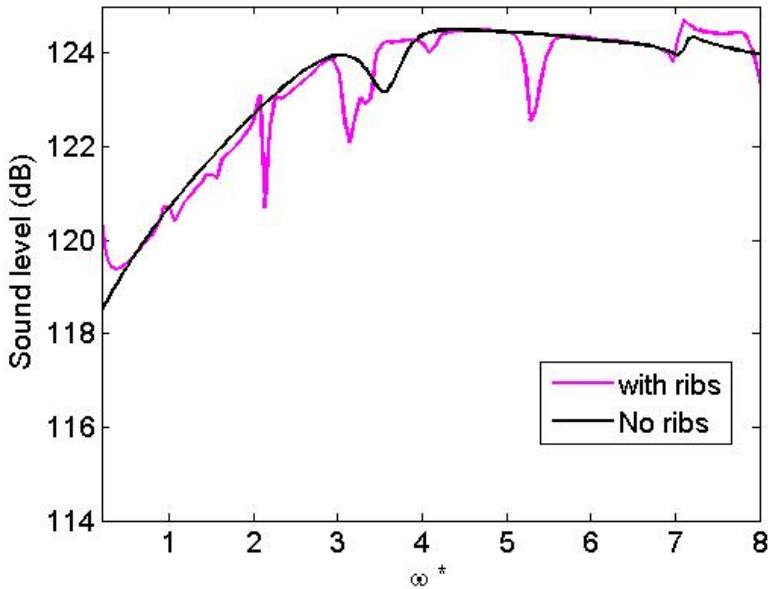

Pressure directivity of an axial dipole located along the duct axis for different materials.

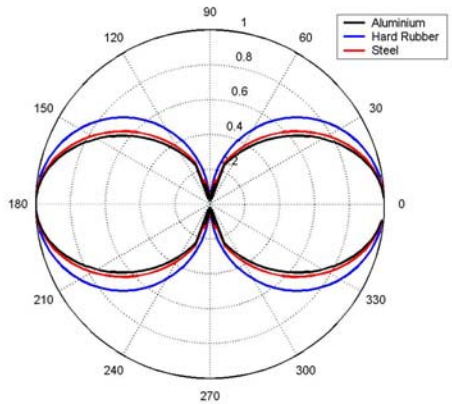

$\omega^* = 0.1$

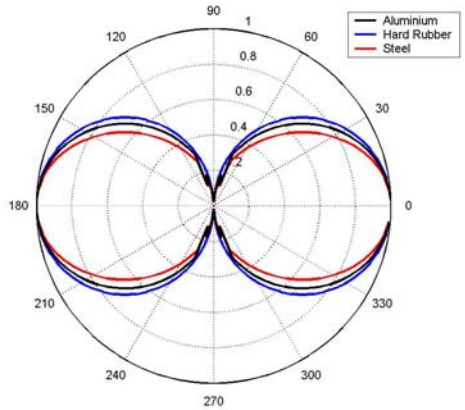

$\omega^* = 1$

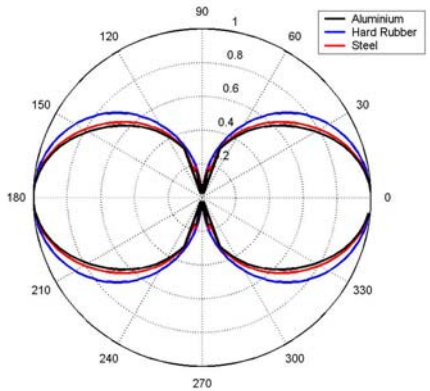

$\omega^* = 2$

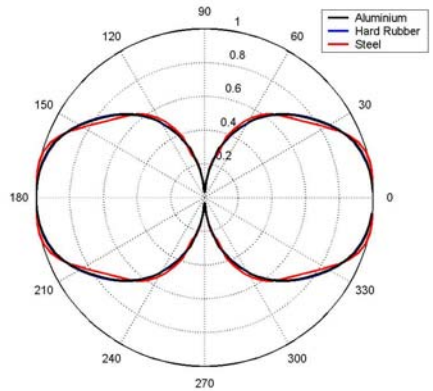

$\omega^* = 5$

Pressure directivity of an axial dipole located at r=0.5a, θ=0, for different materials.

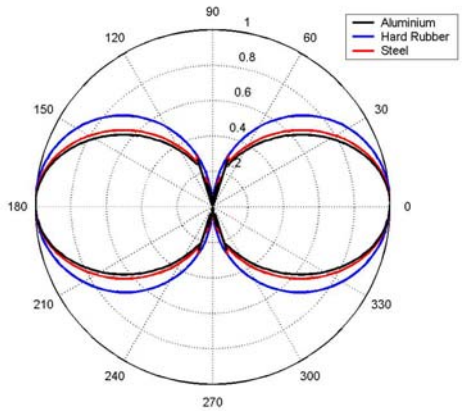

$\omega^* = 0.1$

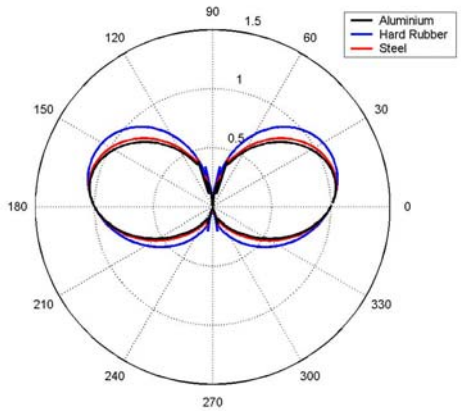

$\omega^* = 1$

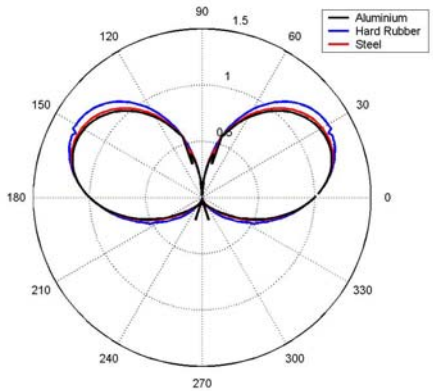

$\omega^* = 2$

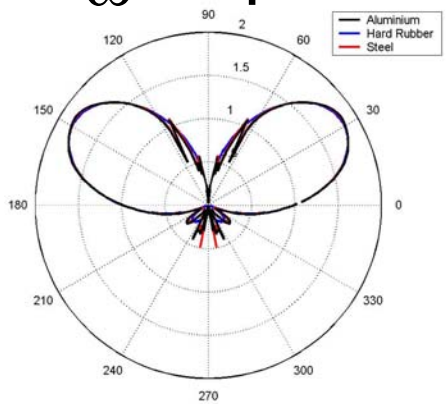

$\omega^* = 5$

Pressure directivity of a radial dipole located along the duct axis for different materials.

$\omega^* = 0.1$

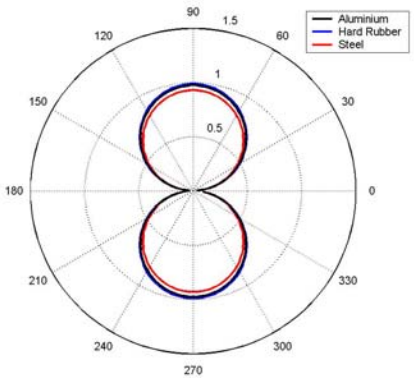

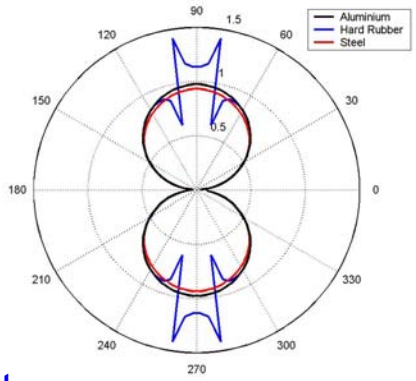

$\omega^* = 1$

Sharp directivity pattern for HR

$\omega^* = 2$

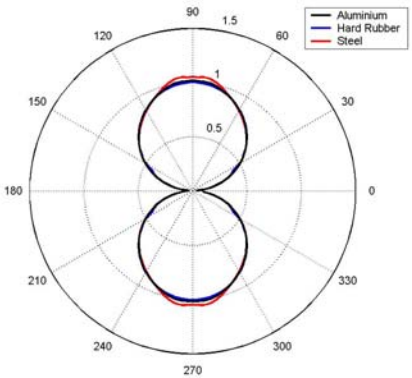

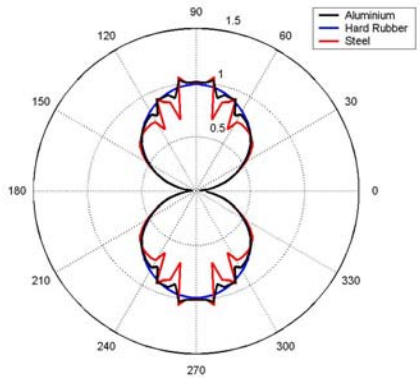

$\omega^* = 5$

Pressure directivity of a radial dipole located at r=0.5a, θ=0, for different materials.

ω* =0.1

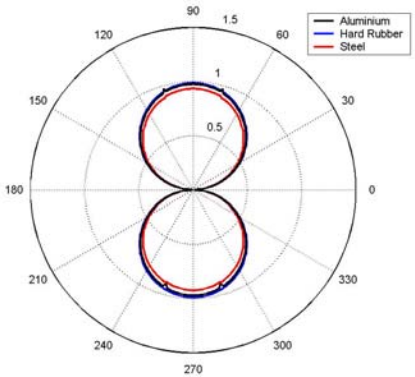

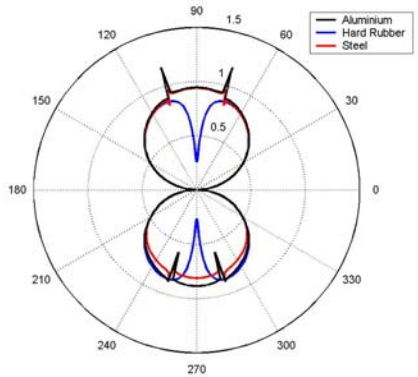

ω* =1

ω* =2

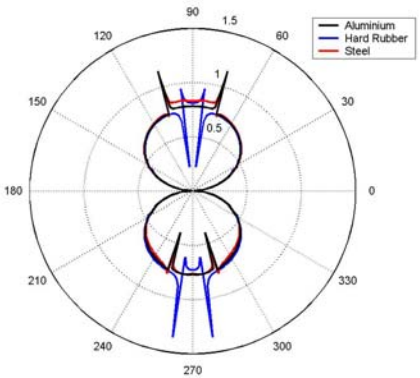

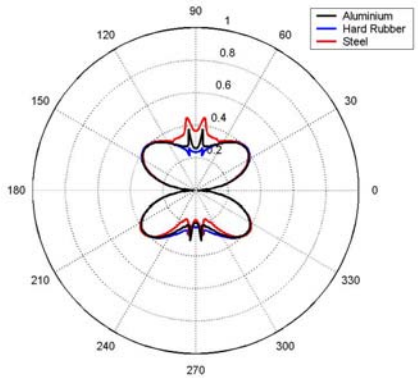

ω* =5

Pressure directivity of a circumferential dipole located at r=0.5a, θ=0, for different materials.

ω* =0.1

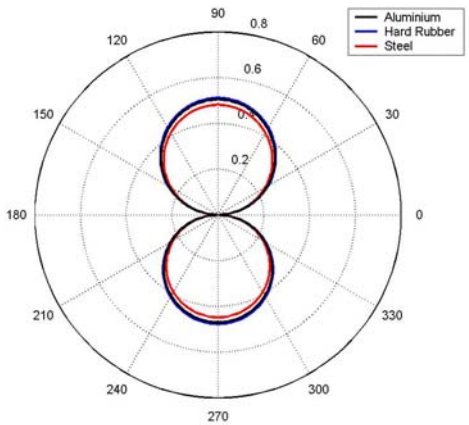

ω* =1

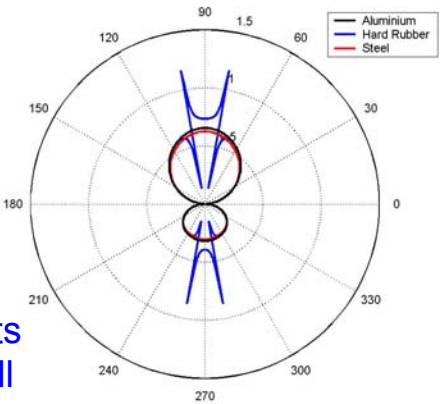

Sharp directivity at high frequency suggesting non-compact source effects due to interaction with shell

ω* =2

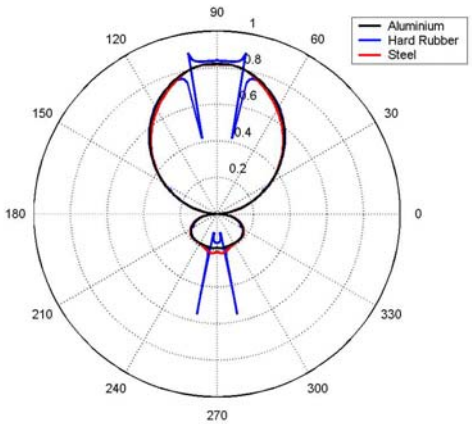

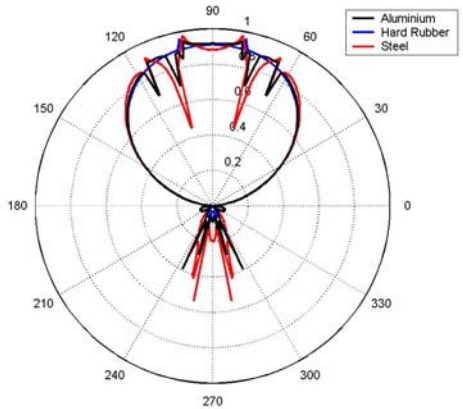

ω* =5

Summary of Single Force and Dipole Results

- The sound power radiated strongly depends on the location and orientation of the force and dipoles, i.e., blade shape, stagger and twist.
- Concentrated single force is a more efficient sound source.
- Circumferential dipoles show strong directivity at moderate and high frequencies suggesting non-compact source effects due to shell excitation.
- Ribbed ducts exhibit sharp variation in sound level and directivity at higher frequencies, suggesting scattering by ribs and greater sensitivity of equivalent sources to shell modes for ribbed ducts.

Rotor Stator Interaction

B=2, V=10, Reduced Frequency =1

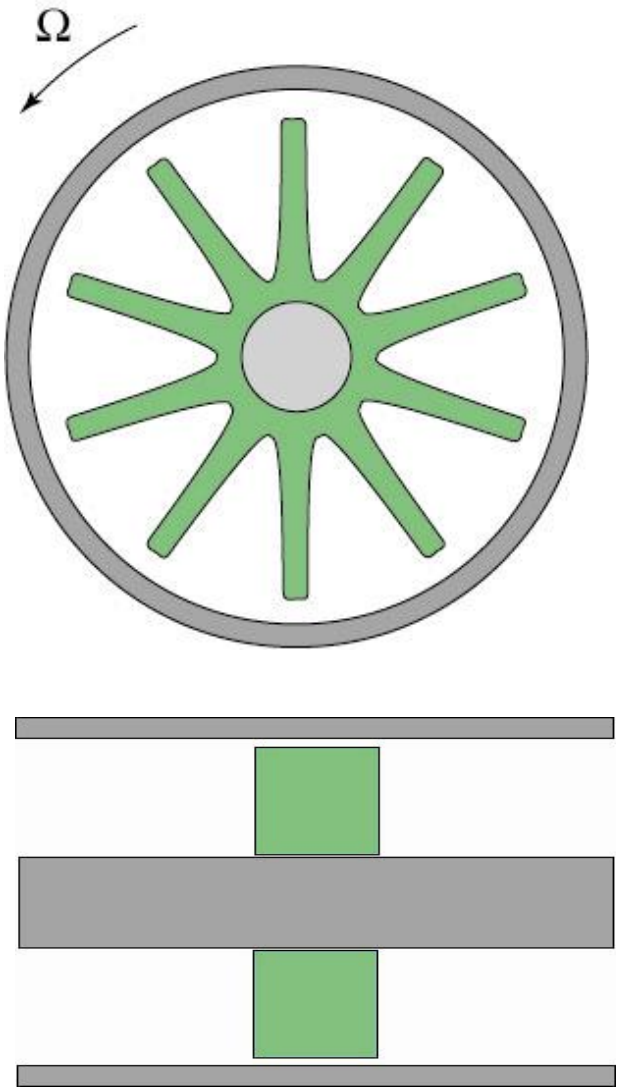

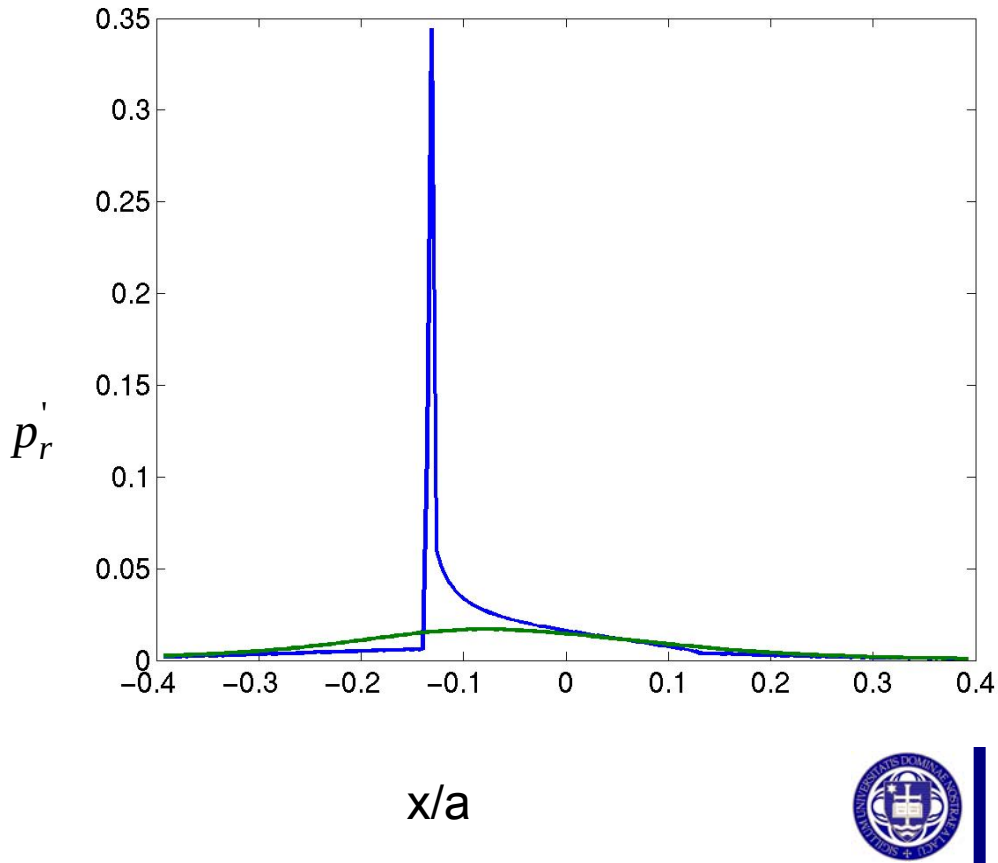

Rigid and flexible aluminum duct wall displacements in response to rotor stator interaction.

B=2, V=10, propagating modes: m= 2, -8, 12

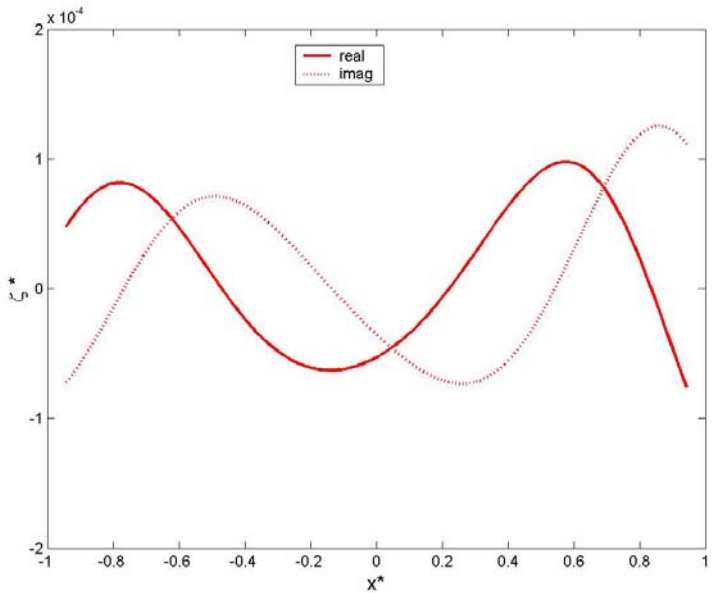

Rigid Duct Excitation

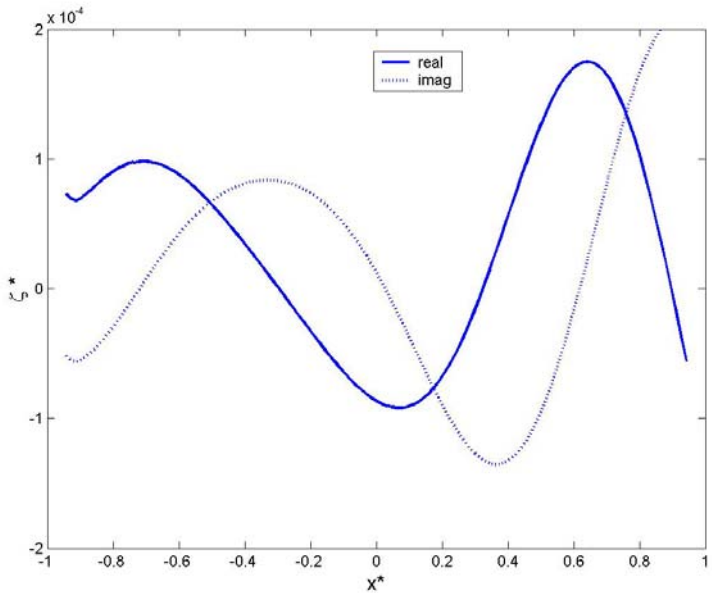

Flexible Duct Excitation

Aluminum Shell Axial and Circumferential Vibrations in Response to Rotor /Stator Interaction Magnified 300 times

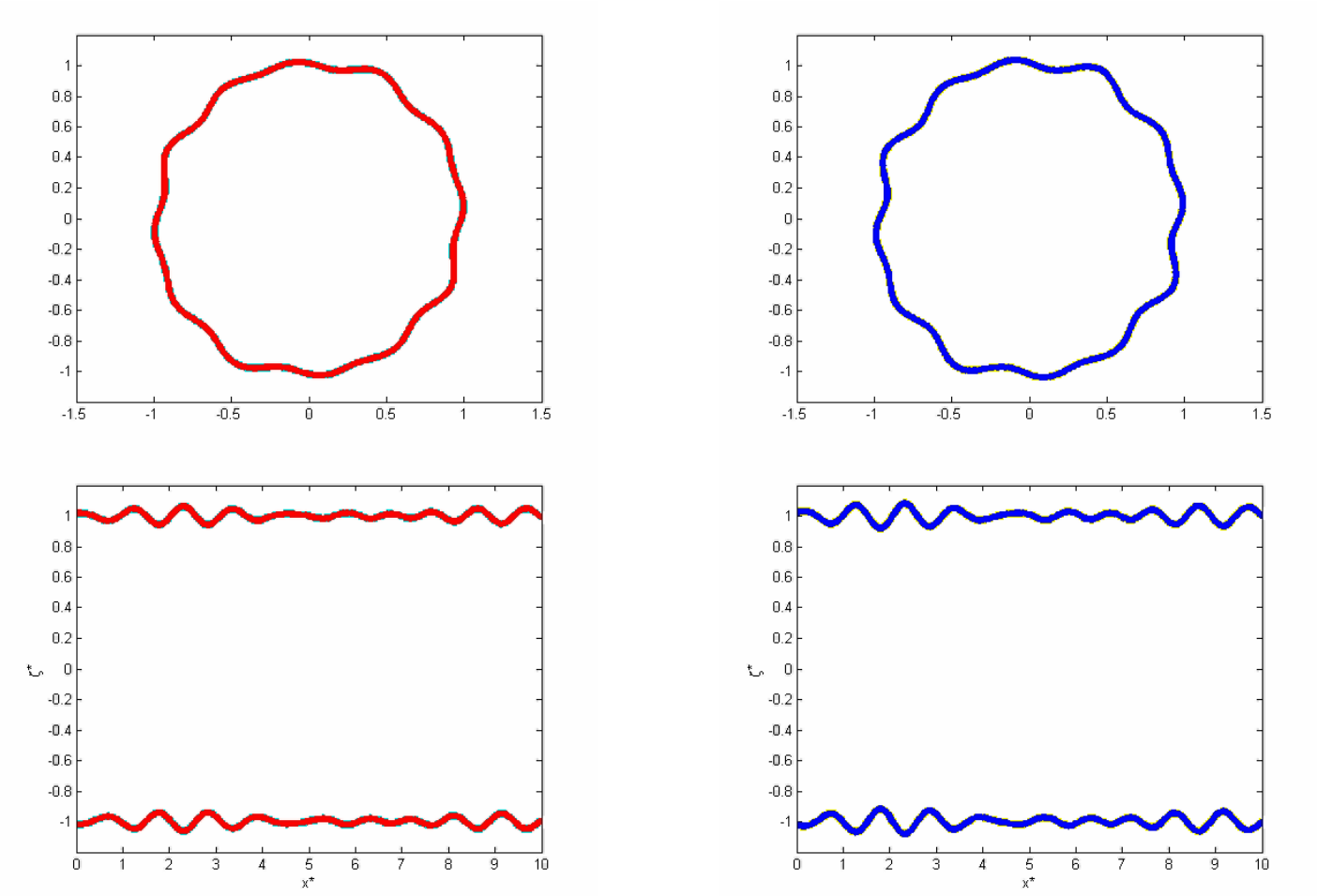

Rigid Duct Excitation

Flexible Duct Excitation

Aluminum duct wall pressure in response to rotor/stator interaction for rigid and flexible ducts – Single blade passage. B=2, V=10, propagating modes: m=2, -8, 12.

Rigid Duct

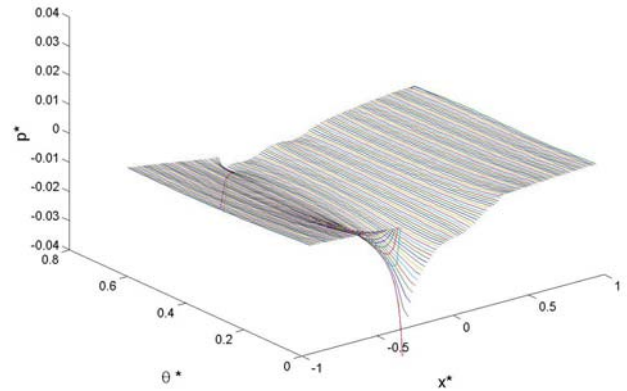

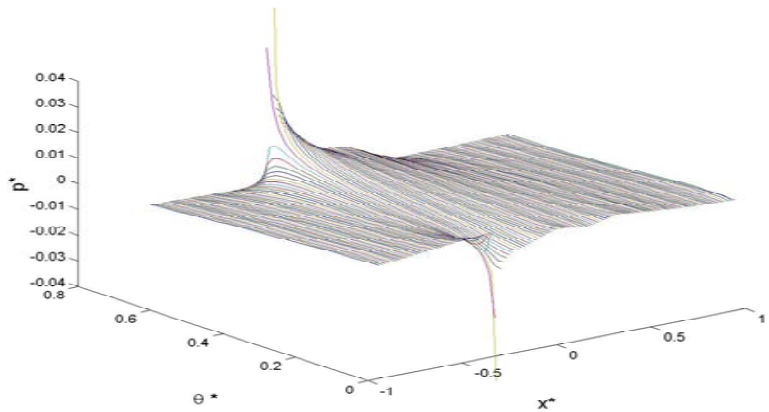

Flexible Duct

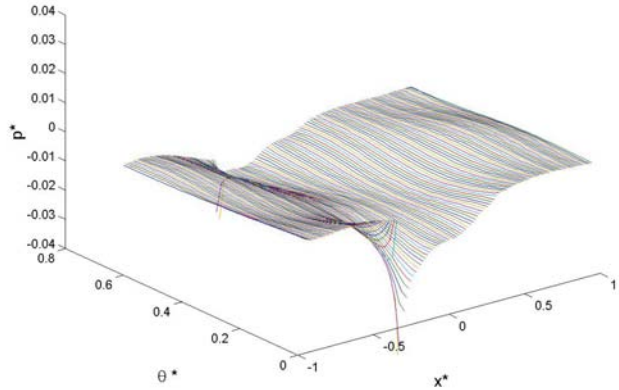

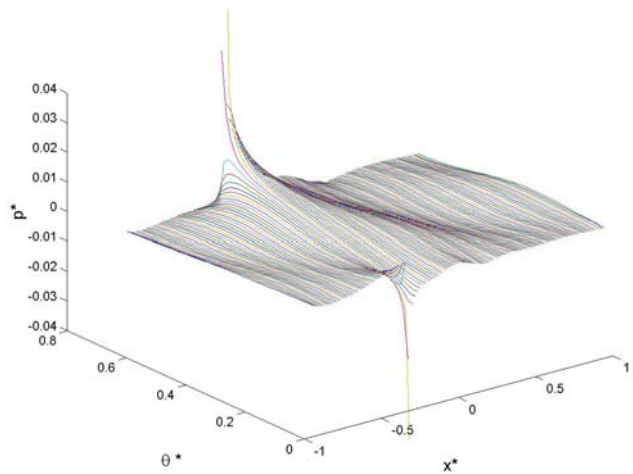

Sound pressure directivity for hard and soft aluminum duct walls normalized to $\rho U u_g$

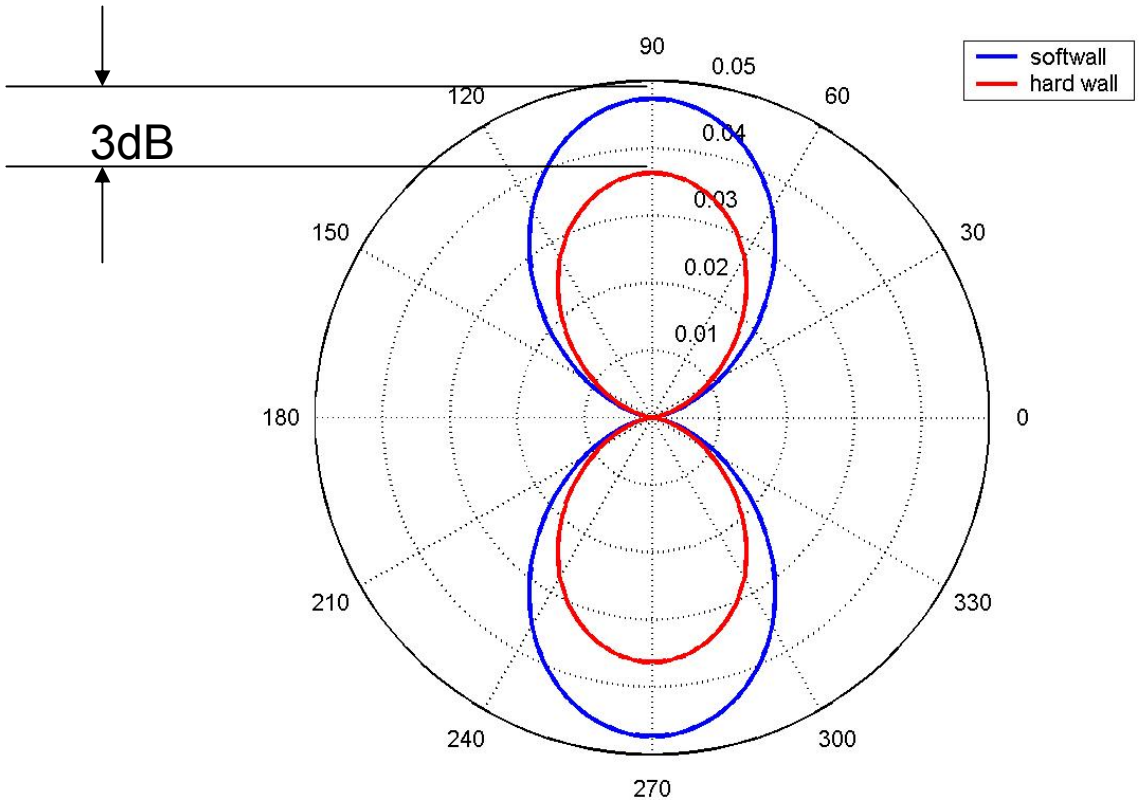

Magnitude of the blade sectional Lift for $\omega^*=1$ for hard and soft walls in response to rotor/stator interaction

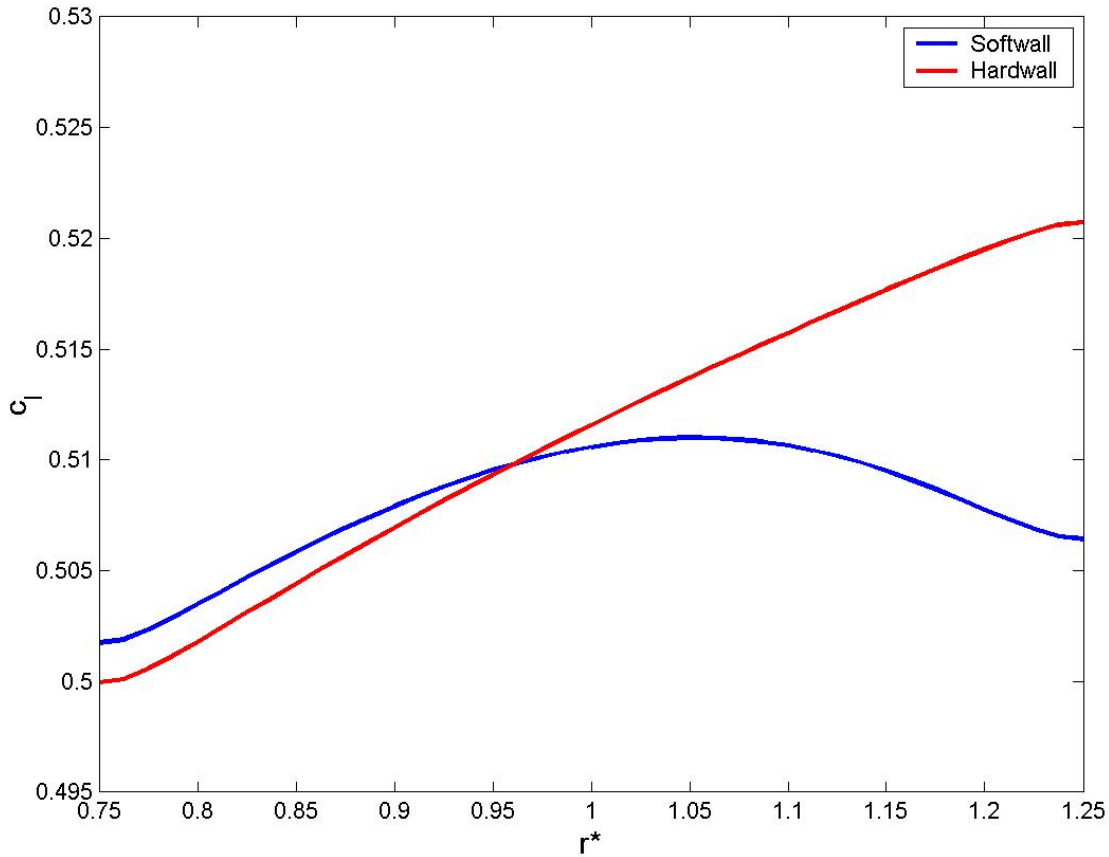

Rigid and flexible "hard rubber" duct wall displacements in response to rotor stator interaction.

B=2, V=10, propagating modes: m= 2, -8, 12

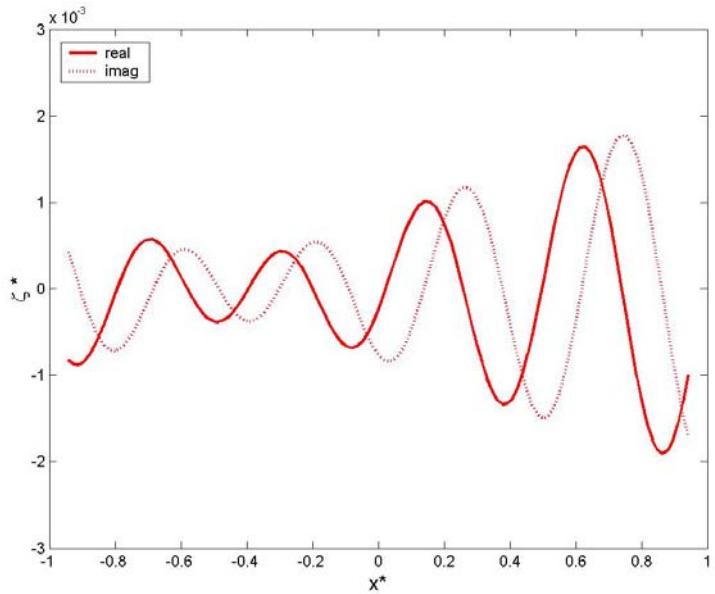

Rigid Duct Excitation

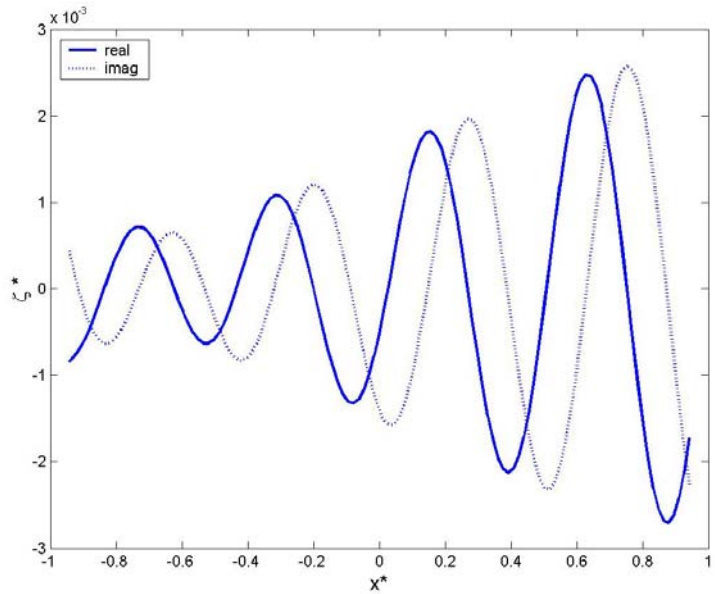

Flexible Duct Excitation

"Hard Rubber" Shell Axial and Circumferential Vibrations in Response to Rotor /Stator Interaction Magnified 50 times

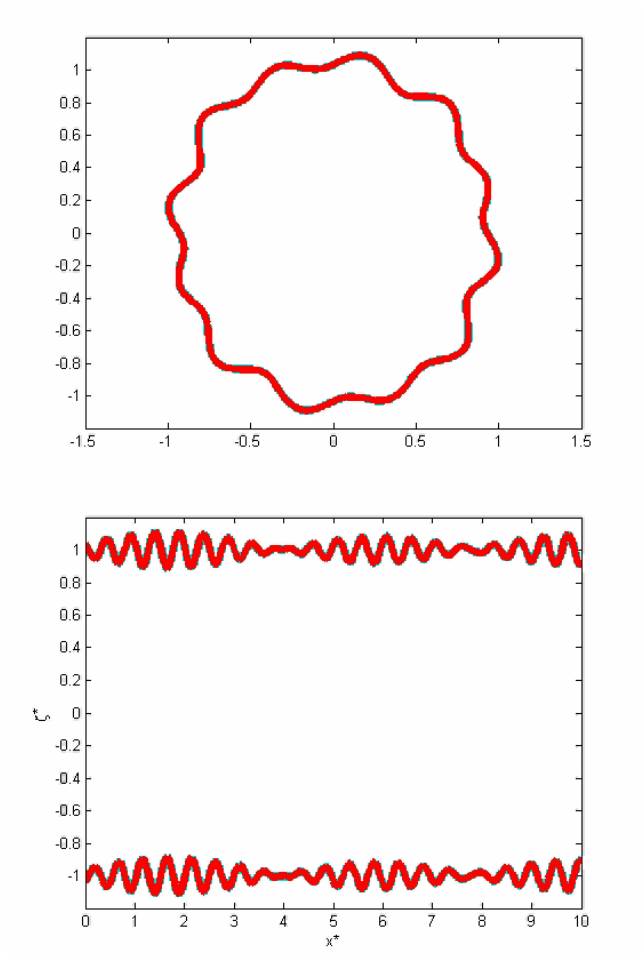

Rigid Duct Excitation

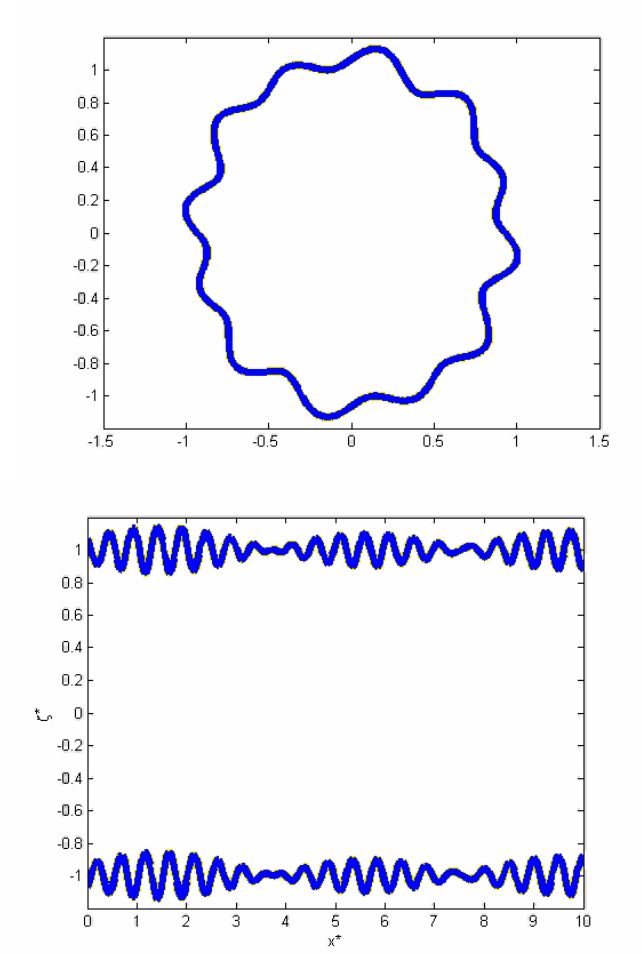

Flexible Duct Excitation

"Hard Rubber" duct wall pressure in response to rotor/stator interaction for rigid and flexible ducts – Single blade passage. B=2, V=10, propagating modes: m=2, -8, 12.

Rigid Duct

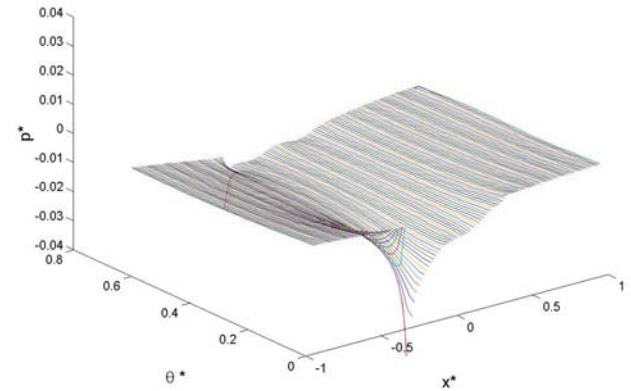

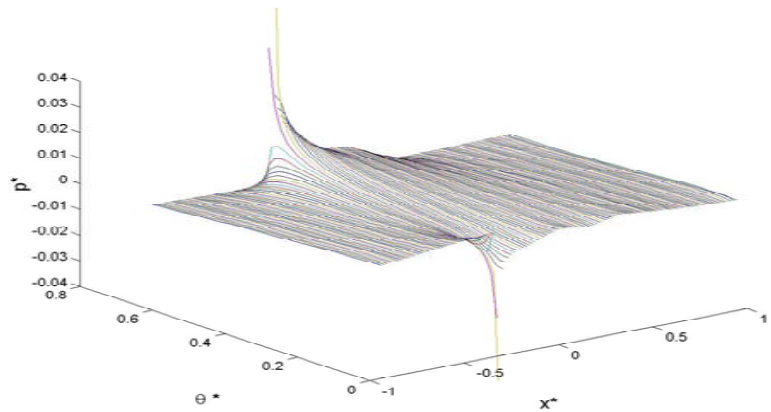

Flexible Duct

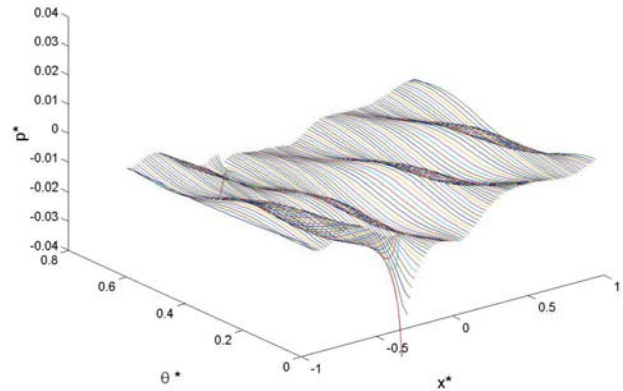

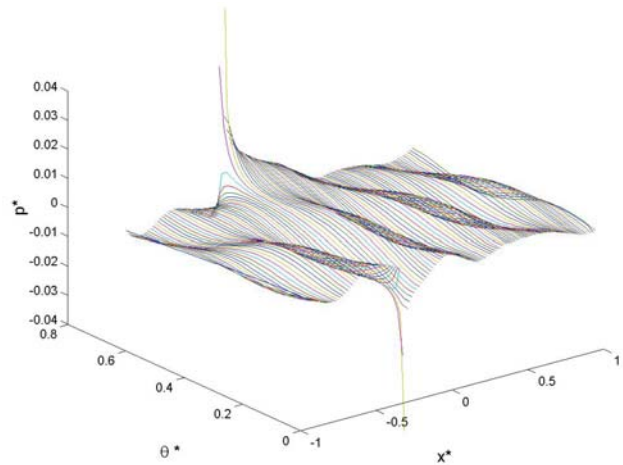

Sound pressure directivity for hard and soft "hard rubber" duct walls normalized to $\rho U u_g$

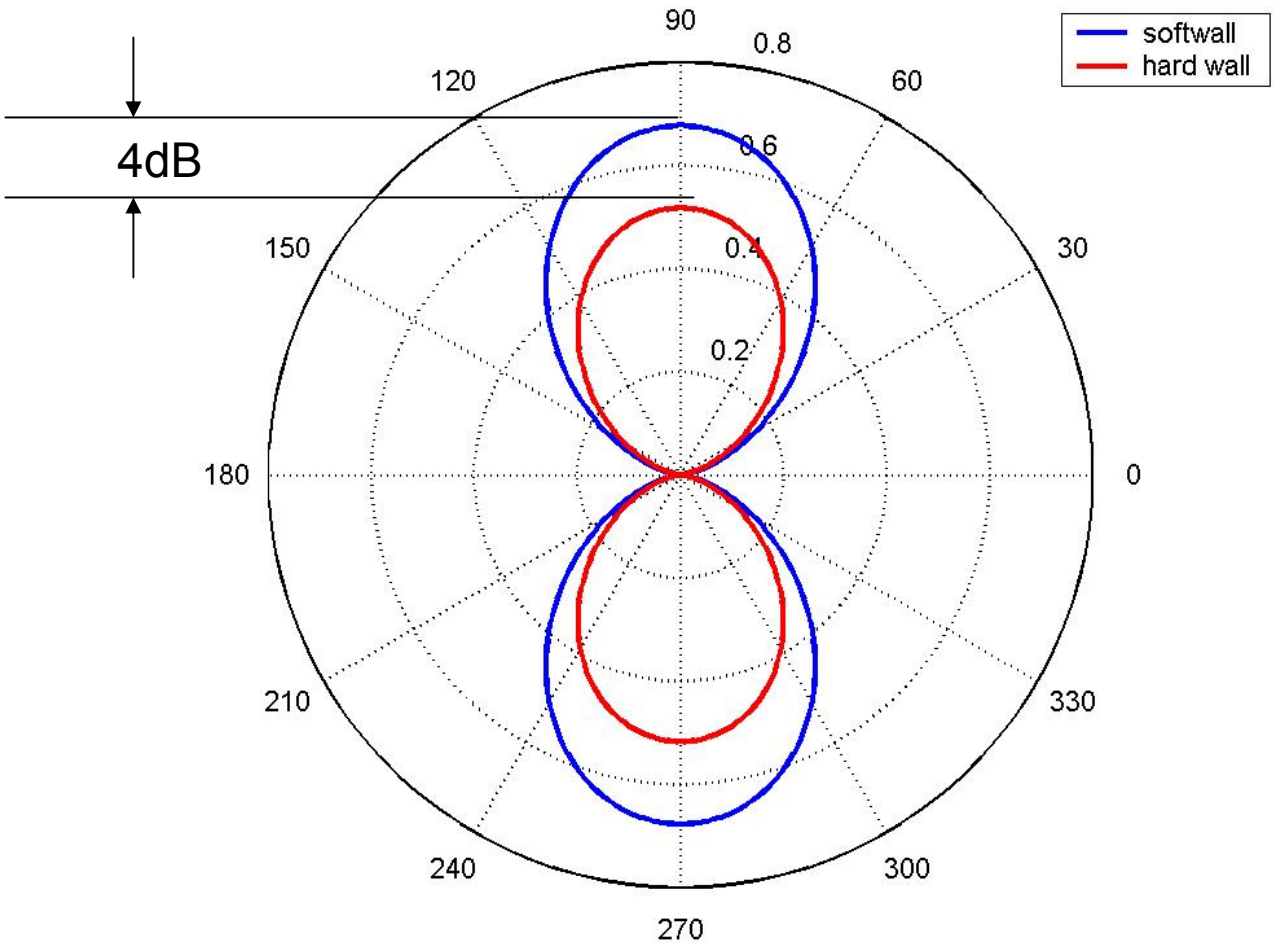

Magnitude of the blade sectional Lift for $\omega^*=1$ for hard and soft walls in response to rotor/stator interaction (hard rubber).

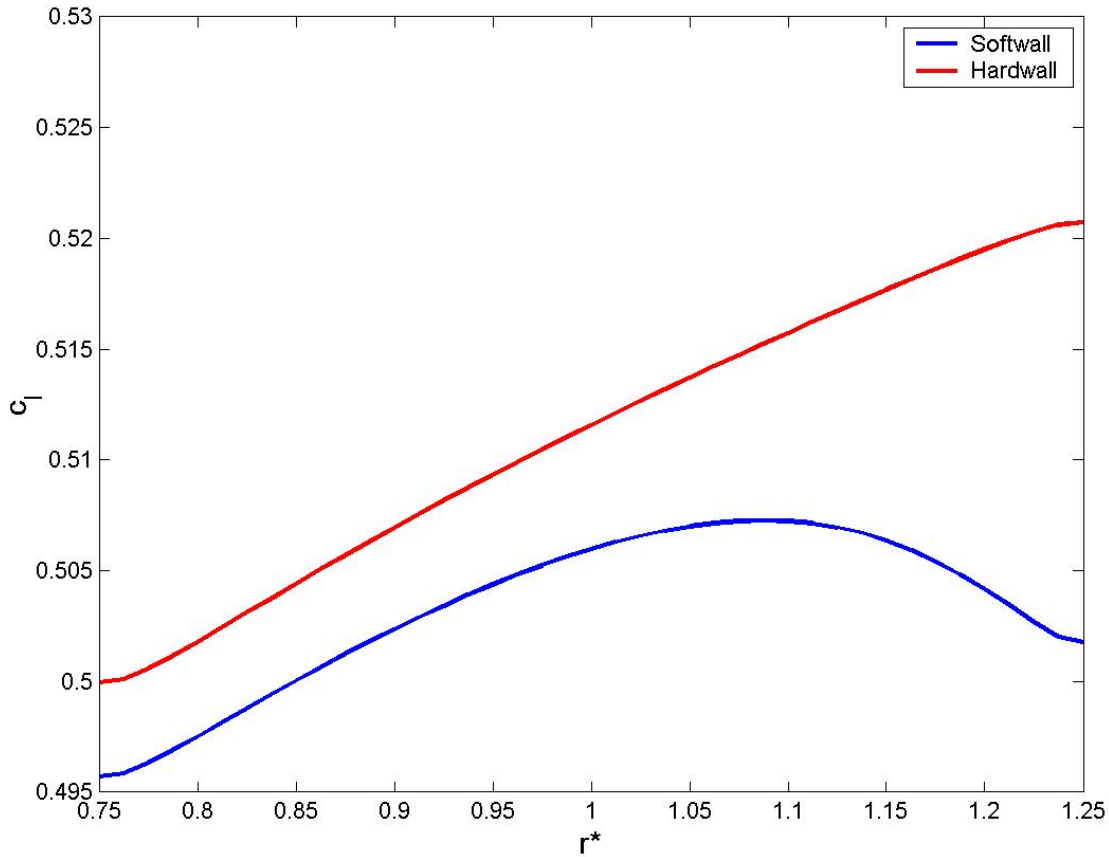

ACCOMPLISHMENTS

- A model is Developed for Fluid-Structure Interactions in Ducted Swirling Flows with ribs:
  - The model identifies, characterizes and quantifies various mechanisms of non-uniform flow-propeller interaction in an elastic flexible duct.
  - The model couples fluid/elastic duct analysis and yields source strength and influence functions as well as acoustic transfer functions.
  - *Thus, the model brings together two classical fields: hydro-acoustics and structural acoustics.*

- Results are presented for plane waves, single forces, dipoles and rotor/stator interaction:
  - The effects of the elastic duct own motion on the blade dipole and acoustic transfer function depend on the level of the duct flexural excitations and in particular on the ratio of the radial oscillatory velocity of the duct to that of the impinging gust.
  - The acoustic radiations are enhanced when the elastic duct-flow system has propagating modes. Such modes are affected by the flow and the duct flexible motion.
  - The presence of the ribs causes strong changes to the dispersion relation and the fluid-structure coupling. The radiated sound exhibits sharp variations and directivity patterns

Significance

- The present method was applied to the rotor/ stator interaction problem and revealed the importance of the duct wall pressure generated by the blade tips as a significant mechanism for noise generation. It was demonstrated that the elasticity of the shell enhances the acoustic sources and adds about 3 to 4 dB to the radiated acoustic power.

- The results suggest that for different combinations of rotor/stator blade counts, it is possible to have a low circumferential modal number (m), which is an efficient radiator of acoustic energy.

- The results also indicate that when free shell modes exist, we have propagating shell modes which force acoustic modes inside the duct and yield higher acoustic radiation outside the duct. *Thus, aluminum will be a much more efficient sound radiator than hard rubber.*

Future Work

- Continue the predictive model development for fluid-structure interactions in ducted swirling flows accounting for coupling the propeller to the elastic duct system.
- Extend the model to ducts with ribs.
- Model the coupled inflow-rotor-stator- duct interaction and examine the contributions of inflow modulated rotor wakes and that of viscous wakes on the velocity aperiodic and periodic modes.
- Analyze the effects of different rotor/stator blade count on the acoustic power radiated.
- Carry out bench mark problems for experimental validation for different excitations such as propagating duct acoustic waves, strong interaction regions(blade tip-duct), blade dipoles in swirling flows, turbulent boundary layer.